Diamond growth by chemical vapour deposition

J J Gracio, Q H Fan, J C Madaleno

Table of Contents

Diamond growth by chemical vapour deposition

J.J. Gracio*, Q. H. Fan and J.C. Madaleno

Nanotechnology Research Division (NRD), Centre for Mechanical Technology and Automation, University of Aveiro, 3810-193, Aveiro, Portugal

* Author for correspondence; electronic mail: jgracio@ua.pt

Abstract

This paper reviews the growth of diamond by chemical vapour deposition (CVD). It includes the following seven parts. 1. Properties of diamond. This part briefly introduces the unique properties of diamond and their origin and lists some of the most common diamond applications. 2. Growth of diamond by chemical vapour deposition. This part reviews the history and the methods of growing CVD diamond. 3. Mechanisms of CVD diamond growth. This part discusses current understanding on the growth of metastable diamond from vapour phase. 4. Characterization of CVD diamond. We discuss two most common techniques, Raman and XRD, which have been intensively employed for characterizing CVD diamond. 5. CVD diamond growth characteristics. This part demonstrates the characteristics of diamond nucleation and growth on various types of substrate materials. 6. Nanocrystalline diamond. In this section, we present an introduction to the growth mechanisms of nanocrystalline diamond and discuss their Raman features.

This paper provides necessary information for those who are starting to work in the field of CVD diamond and as well as for those who need a relatively complete picture on the growth of CVD diamond.

Key words: diamond film, chemical vapour deposition, nanocrystalline diamond

1 Properties and applications of Diamond

A diamond crystal consists of carbon atoms tetrahedrally bonded with sp^3 hybrid bonds. It has a body centred cubic structure as shown in Fig. 1. Choose any characteristic property of a material – structural, electrical, optical or mechanical – the value associated with diamond represents almost always an extremist position among all materials considered for that property. Table 1 lists some of the remarkable properties of diamond. All the exceptional properties of diamond arise from two basic facts:

(1). Carbon atoms are relatively small and light, with short range bonds in the diamond structure.

(2). When the carbon atoms bind together with the diamond structure, they form very strong covalent bonds.

Fig. 1.

Table 1

Due to the high strength of the covalent bond (347 kJ/mole) a lot of energy is required to remove a carbon atom from the diamond lattice, making diamond very hard and abrasion-resistant. In fact, diamond can only be scratched by another diamond or polished by diamond powder. In normal wear the surface of a polished diamond is not scratched by contact with other materials, although the edges can be chipped because diamond is quite brittle.

The atoms in the lattice vibrate according to the normal mode of vibration of the crystal. The vibration frequency is proportional to the restoring force and inversely proportional to the mass of the vibrating atoms. Because the atoms in diamond are both strongly bonded and light, they can vibrate at unusually high frequencies. The maximum frequency is about 40×10^{12} Hz, compared with 16×10^{12} Hz of silicon. The high frequency of vibration results in the diamond fast heat conduction, which is even faster than in metals: at room temperature diamond conducts heat 4 times better than copper.

It is known that vibration quanta or phonons can be created above the fundamental vibration level in a crystal by heat or by infrared radiation. In diamond, photon absorption with the creation of only one

phonon is forbidden by the inversion symmetry of diamond lattice [1]. Absorption with the creation of two phonons is observed at photon energies up to about 2665 cm^{-1} approximately twice the maximum frequency of lattice vibrations [2]. This leads to a high transparency of diamond to most infrared radiation – it is only slightly opaque in mid-infrared wavelength between 4-5 μm, making diamond a promising material for window and detector applications.

Due to the large band gap, about 5.47 eV are required to excite an electron from the valence band to the conduction band, compared with 1.1 eV for Si and 0.7 eV for Ge. Diamond is therefore a wide bandgap material, since 5.47 eV is much higher than the thermal energy k_BT~0.025 eV (where k_B is Boltzmann's constant and T is the absolute temperature) and the probability of thermal excitation of electrons from the valence band to the conduction band is negligible at room temperature. The electric breakdown field is correspondingly high: 2×10^7 V/cm for diamond, and only 3×10^5 V/cm for Si and 4×10^5 V/cm for GaAs.

While diamond possesses a wide bandgap, the band structure calculation and experiments demonstrate that the vacuum level lies below the conduction band and diamond is known to show negative electron affinity (NEA) [3]. This allows the diamond surface to emit electrons to the vacuum with a low applied electric field and opens the door for the use of diamond for cold cathodes and field-emitter displays.

1.1 CVD diamond applications

Even though natural diamonds have been known for several thousand years, they are mainly used as gemstones and as abrasives and cutting tools. In fact, bulk diamond cannot be effectively engineered into the many physical configurations required to exploit all desired combinations of its properties. The development in the synthesis of diamond by chemical vapour deposition (CVD) lead to the ability of growing diamond in the form of thin films or coating on a variety of shapes with controlled grain size and enabled the exploitation of more combinations of the extreme properties of diamond for specific applications. Table 2 lists the properties and application or possible application areas of CVD diamond.

Table 2

Tribological applications come naturally as one of the main and well-established diamond application areas. Diamond-based tools can be divided into two main areas: (i) tools fabricated using conventional powder metallurgy techniques, where diamond particles are mixed and sintered together with a powder metal matrix and (ii) CVD diamond coated tools, where a thin diamond film is deposited on the tool surface. Commercially available diamond-based tools include drill bits, plates, die blanks, grinding and cut-off wheels, blades, chain saws and circular concrete saws (www.idr-online.com). Diamond-coated tools take advantage of diamond's high wear resistance and chemical inertness and can be used for ultra-precision- and micro-machining of nonferrous materials and metal matrix composites, whenever high tolerances and surface finishes are required [4]. In addition, diamond's high thermal conductivity and thermal oxidation resistance make it a suitable material for high speed and dry machining [5] and for the moulding industry [6]. Diamond's wear resistance, together with the range of high transmittance, enabled the use of various diamond coatings on wear-resistant windows [7], UV mirrors [8], IR [9], microwave [10], RF [11] and optical transmission windows [12] and waveguides [13].

Diamond is a wide bandgap material with a large breakdown field and a high hole mobility, characteristics that make it a promising material for high power and high frequency electronic applications. Several diamond-based devices have already been developed, such as transistors operating in the microwave range [14], high-temperature diodes [15], thermistors [16] and transistors [17], laser windows [18] and solid-state detectors [19]. Diamond field emitters and cold cathodes take also advantage of the NEA [20]. The excellent thermal properties of diamond are the basis of heat-spreading films for RF devices thermal management [21] and, more recently, diamond packages for high power lasers [22]. Taking advantage of diamond high stiffness and corresponding high sound velocity, diamond-based surface acoustic wave (SAW) devices [23], micromechanical oscillators [24] and tweeter components [25] have also been successfully developed and commercialized.

In the field of electrochemistry, diamond has again proven to be a unique material. The chemical inertness of CVD diamond makes it extremely resistant to oxidation and attack by acids, even at high

temperatures, and boron doped diamond electrodes have been successfully used in electroanalysis [26] and bulk oxidation of dissolved species in solutions [27]. Diamond electrodes for electrochemical water treatment are a commercial product readily supplied by several organizations, such as CONDIAS and CSEM. These electrodes take advantage of the stability and the chemical inertness of the diamond surface and of the large potentials that can be applied before the water electrolysis takes place.

2 Growth of Diamond by Chemical Vapour Deposition

Deposition of diamond by Chemical Vapour Deposition (CVD) has been largely studied by different research groups worldwide since the early 1980s. This technique involves the deposition of carbon atoms that originate from the dissociation of a carbon-containing gas precursor on a solid substrate. This substrate can be either bulk diamond (either natural or synthetic) or a non-diamond substrate. In the first case, the resulting films are said to be homoepitaxial or singlecrystalline, in opposition to heteroepitaxial or polycrystalline films in the latter case. The deposition of diamond on a foreign substrate usually requires an extra nucleation step, since diamond does not grow spontaneously on non-diamond materials. This step provides the non-diamond substrate with the necessary diamond seeds that grow three-dimensionally until the grains coalesce, forming a continuous polycrystalline film with average grain size increasing with increasing film thickness (van der Drift growth) [28]. The resulting films are poly, nano or ultra-crystalline, depending on the average grain size, and their macroscopic properties depend on parameters such as grain size or sp^3 / non-sp^3 ratio.

This section will outline the development of diamond deposition by CVD and discuss the technological challenges, issues and achievements of depositing diamond films on foreign substrates.

2.1 Development in Diamond Synthesis by CVD

Artificial diamond synthesis by the high-pressure high-temperature (HPHT) method was first reported in 1955 by General Electric [29]. With this conceptually simple method, graphite is converted to diamond by means of applying proper temperature and pressure conditions. At the same time, research was being made in order to deposit diamond from the gas phase. The first documented report of diamond

growth at low pressure was that of W. Eversole in 1954 [30]. He conducted a wide range of sophisticated experiments based on the following reactions:

$$2CO = C_{(diamond)} + CO_2, \quad (1)$$

$$2CO = C_{(graphite)} + CO_2 \quad (2)$$

which are thermodynamically possible due to the negative Gibbs free energy. In these experiments, either diamond or graphite was used as seeds. The experiments were conducted at temperatures from 820 to 1007 ºC and pressures from 5×10^6 to 31×10^6 Pa. It was found that the measured equilibrium ratio CO/CO_2 over diamond (reaction (1)) was different from that over graphite (reaction (2)), which was expected from thermodynamic data, as the equilibrium is different for $C_{diamond}$ and $C_{graphite}$. Furthermore, he found that the equilibrium and the precipitation of diamond on the diamond seed was metastable. No graphite was detected, although under these process conditions (pressure and temperature) graphite was the thermodynamically stable modification. The typical growth rate of diamond over the diamond particles was in the order of 2~3% per hour.

In 1956, the former U.S.S.R. scientists B. Spitsyn and B. Deryagin proposed the growth of diamond at low pressures through the thermal decomposition of carbon tetraiodide [31]. Diamonds were synthesized by using CBr_4 or CI_4 at temperatures ranging from 800 to 1000 °C and pressures of approximately 4×10^{-4} Pa.

The Soviet group subsequently explored direct CVD from hydrocarbons and in 1969 it was stated that diamond was synthesized from pure methane at pressures from 13 to 40 Pa and temperatures from 950 to 1050 °C with a growth rate about an order higher than that reported by Eversole.

A major breakthrough on the CVD diamond process was achieved in the early 1970s. It was the use of atomic hydrogen during growth to remove graphite co-deposits, based on the fact that atomic hydrogen etches graphite much faster than it does diamond. This gave a much higher growth rate and, of equal importance, it permitted the nucleation of new diamond crystallites on non-diamond substrates. The

use of atomic hydrogen was independently pursued by J. Angus in the U.S.A. and by V. Varnin in the U.S.S.R. [32].

The modern era of CVD diamond started in the early 1980s. A Japanese group, the National Institute for Research in Inorganic Materials (NIRIM), first published a remarkable series of papers in which different techniques, hot-filament CVD process, RF-plasma CVD, and microwave plasma CVD were described [33-36]. They reported that diamond particles and films could be deposited on various substrates heated around 850 °C, using a mixed gas of methane diluted by hydrogen, and preferred partial pressures in the range 4×10^3 to 5×10^3 Pa. A growth rate higher than several microns per hour was achieved. These results were soon confirmed by several research groups in the U.S.A. and Europe [30-32].

The success of the NIRIM group was almost immediately spread and spawned numerous research programs in the world. These programs included process techniques, understanding the mechanism of CVD diamond nucleation and growth, diamond doping, investigation of optical, electronic, thermal, mechanical properties of CVD diamond, diamond coating on various substrates for specific applications, characterization of CVD diamond, etc.

2.2 CVD systems

The growth of diamond films from vapour phase on non-diamond substrates at practical rates was accomplished with the development of thermal- and plasma-enhanced CVD methods, in which a hydrocarbon gas (usually methane) mixed in low concentrations with hydrogen is energized thermally or in a plasma, prior to contact with a heated substrate. The first of these enhanced CVD methods was the chemical transport reaction synthesis developed by Soviet workers in the late 1970s [37,[38]. From that time until the late 1980s, virtually all of the significant developments reported have been due to Japanese work. These include the development of filament-assisted thermal CVD [33,34], electron-assisted thermal CVD [39,40], laser-assisted thermal CVD [41], RF-plasma CVD [42], microwave-plasma CVD [35], combustion flame-assisted CVD [43], direct-current arc plasma jet CVD [44], etc.

The various enhanced CVD methods, although different in their process details, have a number of common features, the most important of which are the following:

(1). Growth in the presence of atomic hydrogen

The deposition of polycrystalline diamond films from carbon containing species in the presence of atomic hydrogen was based on the realization that diamond is more stable towards atomic hydrogen than graphite. More specifically, if two neighbours of a carbon atom in the diamond structure are replaced by hydrogen, the sp^3 hybridization is still maintained, while a similar operation in graphite alters the electronic bonds in the whole graphite ring. Thus, growth of diamond from carbon containing molecules diluted in hydrogen involves two processes. The first is carbon deposition primarily in the form of graphite with a small amount of diamond, and the second is selective etching of graphite by atomic hydrogen. As a result, the various enhanced CVD methods for the growth of diamond are optimized to produce atomic hydrogen from molecular hydrogen close to the surface of the growing film.

(2). Dissociation of carbon-containing source gases.

In a simple thermal CVD process, the diamond growth rate is very low (<0.1 μm/h). This is due to the rather high activation energy needed for the decomposition of methane on the surface of diamond (230-243 kJ/mol). Thus, in the various enhanced CVD methods, the carbon-containing compounds are dissociated by thermal, plasma or combustion processes to produce the reactant species responsible for the diamond nucleation and growth. The film growth rate depends on the ability of these reactant species to be transported to the substrate.

(3). Growth at moderate substrate temperatures

In all enhanced CVD methods, diamond growth takes place at substrate temperatures between 500 and 1200 °C. Growth at temperatures above or below this range often leads to graphite or diamond-like-carbon (DLC) deposits, respectively. In the following section, we briefly introduce several CVD methods which are commonly used for the growth of diamond films.

2.3 Filament-assisted thermal CVD

A schematic diagram of this deposition method is shown in Fig. 2, and Table 3 outlines the deposition parameters range reported by various works. In this method, diamond particles or films are deposited on a heated substrate from a mixture of methane and hydrogen dissociated by hot tungsten or other high-melting-point metal filament placed close to the substrate. The filament temperature may reach around 2200 ºC during this process. The main role of the hot-filament is to dissociate molecular hydrogen into atomic hydrogen. At higher pressure (3 – 4 kPa) the dissociation mainly occurs near the filament (without adsorption and desorption) due to the high gas temperature. At lower pressure the filament surface acts as a catalyst for adsorption of molecular hydrogen and desorption of atomic hydrogen. The dissociation equilibrium is governed by thermodynamics. Detailed plasma studies have been conducted in order to elucidate the diamond growth mechanism, revealing the presence of different species in the plasma, such as neutral molecules, ions and electrons [45-47].

Fig. 2.

Table 3

Besides the original role of the tungsten filament, it was discovered that during diamond deposition the tungsten filament reacts with methane and undergoes carburization. This results in consumption of carbon from the methane, and thus a specific incubation time is needed for the nucleation of diamond films. Therefore, this process may affect the early stages of thin film growth. In addition, the resistance of the filament should be monitored and adjustments to the supplied voltage and current made in order to maintain the temperature of the filament constant.

Due to the temperature upper limit of the filament material, hot-filament processes operate at significantly lower gas temperatures than plasma processes, and consequently produce less atomic hydrogen. The low gas phase concentrations give relatively low growth rates compared to the plasma methods. Despite these drawbacks, hot-filament assisted deposition has remained popular because of its

low capital cost and simplicity. Also, hot-filament reactors are directly scalable to large sizes and can be used to coat complex shapes and internal surfaces.

2.4 Plasma-enhanced CVD methods

Alternative methods of diamond growth involve various forms of plasma-assisted CVD using carbon-containing species mixed in low concentration with hydrogen. Plasma is generated either by various forms of electrical discharges or by induction heating. The role of the plasma is to generate atomic hydrogen and to produce proper carbon precursors for the growth of diamond. Atomic hydrogen is produced by electron impact dissociation of molecular hydrogen. Although the binding energy of molecular hydrogen is 4.5 eV, electron energies in excess of 9.5 eV are required due to the mass difference between electrons and molecular hydrogen. In fact, such dissociation of molecular hydrogen peaks at electron energies of 25 eV [48]. Thus, atomic hydrogen produced in plasmas generally has high kinetic energy due to the difference between the hydrogen dissociation energy and the electron kinetic energy. This is to be contrasted with the thermal-assisted CVD process, where the produced atomic hydrogen has low kinetic energy.

Similarly, electron impact dissociation processes are responsible for the formation of carbon-containing neutral and ionic radicals. In general, 1% of the molecules in plasma are converted into neutral radicals and about 0.01% into ions. Neutral molecules, for example, CH_4, usually do not participate in the growth of diamond due to a relatively high Gibbs free energy in the process of their decomposition. Thus, the growth rate of the diamond film is mainly determined by the concentration of neutral radicals. The effect of the ionized radicals is not clear. Although their contribution to the growth rate is minimal, one can not rule out ion-assisted processes. For example, Stoner *et al.* reported an enhancement in the diamond nucleation density by microwave plasma-assisted CVD on negatively biased silicon substrates [49].

The absolute concentration of atomic hydrogen and neutral radicals depends on the pressure of the plasma. In low-pressure plasma, the electrons acquire high kinetic energies from the electric field;

however, due to the high mean free path, they do not transfer much energy to molecular species. As a result, the gas temperature is relatively low and thus atomic hydrogen and neutral radicals are produced in low concentrations by collisions with high-energy electrons only. This is to be contrasted with high-pressure plasmas, where, due to the small electron mean free path, the gas and electron temperatures are about the same. Thus, the concentration of atomic hydrogen and neutral radicals is much higher, since both electron and molecular collisions contribute to their formation. This accounts for the significantly higher growth rates reported in high-pressure plasmas.

Among the plasma-enhanced methods, microwave-plasma-assisted CVD has been used much more extensively than others for the growth of diamond films. Fig. 3 demonstrates a typical microwave-assisted CVD system.

Fig. 3.

This method of diamond growth has a number of distinct advantages over the other methods. Microwave deposition, being an electrodeless process, avoids contamination of the films due to electrode erosion. Furthermore, the microwave discharge at 2.45 GHz, being a higher frequency process than the RF discharges at 13.5 MHz, produces higher plasma density with higher energy electrons. This should result in higher concentrations of atomic hydrogen and hydrocarbon radicals. An additional advantage is that the plasma is confined in the centre of the deposition chamber in the form of a ball and this prevents carbon deposition on the walls of the chamber.

2.5 Combustion-flame-assisted CVD

This method allows the growth of diamond at atmospheric pressures using combustion flames from an oxygen-acetylene brazing torch. Because of its simplicity and low cost of the experimental apparatus as well as the high growth rate, this method has been widely used in diamond growth.

A schematic diagram of the apparatus is shown in Fig 4a [30]. It consists of an oxygen-acetylene brazing torch supplied with oxygen and acetylene controlled by a mass flow system and a water-cooled substrate. The substrate temperature is adjusted by varying the substrate surface position relative to the

water cooled copper mount and its temperature is measured by a two-colour pyrometer which is insensitive to the flame's emission. Hydrogen addition to the oxygen-acetylene flame was found to reduce the amount of amorphous carbon in the diamond films [50]. Normally the oxygen acetylene torch is used with an excess of oxygen. The acetylene is completely burned to CO_2 and H_2O. With oxygen depletion, deposition of carbon (normally graphite) occurs. There is a very distinct concentration ratio of C_2H_2/O_2 where this change from carbon deposition and no deposition occurs.

Fig. 4.

Combustion flames operating in the fuel-rich mode have three distinct regions, as shown in Fig. 4b. The inner cone is the primary combustion zone followed by a diffused intermediate region and an outer zone. The temperature in the primary combustion zone can reach up to 3300 K. The main combustion reaction at this region leads to the formation of CO and H_2 (eq. (3)):

$$C_2H_2 + O_2 \rightarrow 2CO + H_2 \qquad (3)$$

with a number of reactive intermediates (H, OH, C_2, C_2H, etc.). In the fuel-rich mode, the un-burnt hydrocarbons as well as the combustion products form the diffuse intermediate and reaction free region (called feather). The outer zone, which is also known as a secondary combustion zone, consists of a flame caused by molecular or turbulent diffusion of oxygen from the surrounding atmosphere. In this region, the products of the combustion reaction are oxidised to CO_2 and H_2O. The substrate is usually placed in the feather region of the flame, where there is an abundance of atomic hydrogen and hydrocarbon radicals as revealed by *in-situ* diagnostic studies [51].

2.6 DC plasma jet CVD

A plasma jet, or "arcjet", is a generic expression for a high pressure direct-current plasma discharge in which convection plays a significant role in transport processes. Fig. 5 presents a typical arcjet used as a source for diamond CVD [30].

Fig. 5

Electrical energy is converted to thermal and kinetic energy of a flowing gas mixture by an electric arc discharge. Like other CVD methods, a major constituent of the gas mixture is hydrogen, while methane is most often introduced into the plasma jet to provide a source of carbon. The plasma temperature is sufficiently high (1000-5000 K on average) to partially dissociate the gas. The plasma jet containing these reactive species impinges onto a cooled substrate surface (T_s~1000-1500 K) for film growth. Normally, the electric discharge is sustained between a concentric cathode rod and a surrounding cylindrical anode, creating an arc column that is nearly fully-ionized. Positive current flows from the anode to the cathode, establishing the voltage drop required to dissipate the total power in the arc.

Extremely high diamond growth rates, ~1 mm/hour, have been achieved using DC arcjet CVD method [52]. In addition, arcjets have a distinct advantage over other diamond CVD methods in that the deposition of diamond can proceed simultaneously with the deposition of other ceramics and metals by introducing powders of various types into the plasma stream. Using this approach, Kurihara *et al.* [53] deposited well adherent diamond films on tungsten-molybdenum substrates by spraying an interlayer composed of tungsten carbide, followed by a composite diamond-tungsten-carbide intermediate layer. Such a functional gradient material reduced the thermal stress between the diamond film and the substrate and increased the adhesion strength by an order of magnitude over that which was obtained in the absence of the tungsten-carbide interlayer.

As a summary, Table 4 provides the basic features of the most commonly used methods for diamond CVD at low pressure.

Table 4

3 Mechanisms of CVD Diamond Growth

The complex chemical processes occurring during the CVD diamond are fascinating and exciting from many perspectives. First, how does one understand the process of growing a material under conditions in which it is metastable, e.g. what are the complex gas phase, surface and bulk chemical processes which lead to diamond *vs.* graphite or amorphous carbon?

Secondly, this process deals with many fundamental aspects of CVD, such as gas phase chemistry, complex heat and mass transport, nucleation, surface chemistry, bulk chemistry and diffusion, and temporal dynamics as shown in Fig. 6. Understanding the effects of a combination of these features is full of challenge. And finally, the technological impact and applications enabled by diamond materials are important in many ways for society and the economy. Industry is already using CVD diamond in applications such as cutting tools, electronic thermal management, optical windows and radiation detectors, as has been introduced before.

Fig. 6

The growth of a solid material from gaseous reactants is fundamentally a surface chemical process which depends on the flux of reactant species to the surface, and products from it, as well as the surface structure and temperature. For diamond CVD, some general features are summarized as follows.

(1). Gas dissociation.

It is essentially required for achieving appreciable diamond growth rates. Dissociating the gas prior to deposition increases diamond growth rates from Å/h to μm/h. Electric discharge, microwave, RF, DC, hot (>2000 °C) filament, and combustion are most commonly used for gas dissociation. Chemical dissociation in halogen-containing systems may be possible at relatively low temperatures.

(2). Independence of dissociation method.

Good quality CVD diamond has been produced utilizing a variety of the above described methods. The ease with which diamond is grown depends on the method, but generally accepted explanations for this influence have not been established.

(3). Independence of carbon-containing precursor.

The chemical nature of the carbon-containing precursor does not determine whether diamond can be grown. Diamond of similar quality and morphology has been grown using a variety of species such as aliphatic or aromatic hydrocarbons, alcohols, ketones, carbon monoxide and halocarbons [54].

(4). Hydrogen is required for efficient growth.

Deryagin and co-workers and Angus first proposed that atomic hydrogen had to be present. Hydrogen in excess of that introduced as part of a hydrocarbon precursor gas may not be needed.

(5). Oxygen enhances the quality of CVD diamond.

Oxygen added in small amounts to hydrocarbon precursor mixtures enhances the quality of diamond deposits. Conflicting results are reported on the effect of oxygen on diamond growth rates.

(6). Diamond precursor species.

The most abundant carbon-containing precursors in typical diamond growth systems are methyl radicals and acetylene molecules.

(7). Co-deposition of diamond and non-diamond carbon.

Graphite and other non-diamond carbons usually deposit simultaneously with diamond.

(8). Diamond growth rate maximum with temperature change.

This maximum occurs around 1000 °C.

(9). Lowering of the growth temperature using halogenated precursor gases.

The addition of halogenated gases to the standard hydrogen and methane vapour phase allows the deposition of diamond films at considerably lower temperatures (250-750 ºC) [55-57].

(10). Substrate surface treatments.

A substrate pre-treatment of scratching with submicrometer diamond powder is common to enhance nucleation rates and densities. Electrical biasing of substrates or ultrasonic treatment can also influence nucleation rates.

(11). Crystallite morphology.

Octahedral {111} and cubic {100} faceted surfaces dominate CVD diamond crystallites, and twinning frequently occurs on {111} surfaces. Cubo-octahedral crystals composed of both {111} and {100} surfaces are also common.

In the following section, we present the current understanding of some critical aspects in diamond CVD growth, including the gas-phase environment, the growth species, diamond doping, diamond surface chemistry, diamond growth mechanism, and diamond quality.

3.1 The gas-phase chemical environment

To understand diamond CVD, it is first necessary to characterize the chemical environment that the diamond film is exposed to during growth. In many other CVD processes this is straightforward, since the pressure is low enough that gas phase chemistry is negligible (low-pressure CVD of polysilicon) or is limited to a few precursor decomposition reactions (organometalic CVD of GaAs). However, in diamond CVD, free radicals – particularly atomic hydrogen – play crucial roles. The presence of radicals ensures that gas-phase chemistry is an integral part of diamond CVD. A mixture of radicals, molecules, and in some cases ions, impinges on the substrate and contributes to the growth of diamond, even though the feed gas composition may be a simple methane/hydrogen mixture.

There have been many studies of the gas-phase chemistry during diamond CVD [58-68]. These investigations revealed that atomic hydrogen and hydrocarbon are perhaps the most critical determinants of CVD diamond as well as its quality and growth rate.

3.1.1 Atomic hydrogen.

The production mechanisms, loss mechanisms and concentration profiles of atomic hydrogen are the basic subjects.

In plasma-enhanced systems such as microwave, RF or DC arcjet reactors, H is produced homogeneously in the plasma. The external energy input couples directly to the free electrons in the plasma. The energetic electrons may directly produce H through

$$H_2 + e^- \rightarrow H + H + e^- \qquad (4)$$

while the dissociation of molecular hydrogen by electrons with energy below than 12 eV may occur via electronic excitation according to Stibbe and Tennyson [69].

In hot-filament systems, at pressures about 4 kPa the dissociation of hydrogen occurs mainly in the gas phase. The atomic hydrogen produced diffuses rapidly away from nearby the filament, resulting in a concentration profile near the filament [70].

The steady state level of atomic hydrogen in the reactor is determined by a balance between the H atom production rate and the destruction rate due to homogeneous chemistry and wall recombination. For typical diamond CVD conditions, homogeneous recombination of H is a slow process, and H atoms are able to diffuse to the walls or to the substrate before recombining in the gas. The rate of the direct recombination reaction,

$$\mathrm{H + H + M \rightarrow H_2 + M}, \qquad (5)$$

is pressure-dependent, due to the need for a third body (M) to carry away the excess heat of recombination. At 20 Torr, the characteristic time for this reaction is in the order of 1 sec [59,60]. In time t an atom may diffuse a distance of order $\sqrt{Dt}$, where D is the diffusion coefficient. Using $D = 0.12$ $\mathrm{m^2/s}$ for H in H_2 at 20 Torr implies a diffusion distance of 35 cm in 1 sec. Therefore, since the substrate is usually at most 1-2 cm from the location of H production, H atoms in an H_2 background are able to freely diffuse to the substrate without homogeneous recombining.

In the presence of a small amount of hydrocarbon, a second path competes with reaction (5) and, in many cases, dominates the homogeneous recombination rate. This is due to the two reactions

$$\mathrm{H + CH_3 + M \rightarrow CH_4 + M} \qquad (6)$$

and

$$\mathrm{H + CH_4 \leftrightarrow CH_3 + H_2}. \qquad (7)$$

Accounting for these and similar reactions, Goodwin and Gavillet [60] have shown from numerical simulations that the homogeneous recombination time is reduced to about 50 ms for a gas composition of 0.5% CH_4 in H_2. However, this still implies a diffusion distance of 8 cm. Therefore, homogeneous recombination of H may be neglected under typical low pressure CVD conditions. Note, however, that at hydrocarbon concentrations of several percent, gas-phase H profiles are affected by the presence of the hydrocarbons, indicating a contribution from homogeneous recombination [70].

Since homogeneous recombination of H atoms is usually negligible, the loss of H atoms must occur primarily on reactor walls and on the diamond surface itself. Measurements of the H concentration profile near a diamond substrate clearly show that diamond is a sink for H at typical substrate temperatures [71].

3.1.2 Hydrocarbon chemistry

The first hydrocarbon concentration measurements during diamond growth were made by Celii *et al.* [58], who used infrared diode laser absorption spectroscopy to detect acetylene (C_2H_2), the methyl radical (CH_3) and ethylene (C_2H_4) in a 3.3 kPa hot-filament reactor with an input gas of 0.5% methane in hydrogen. Later, a similar measurement was also made for a 2.7 kPa microwave system [72]. The measured acetylene concentration represented conversion of 10-20% of the initial methane. Since the gas-phase conversion of methane to acetylene requires several sequential reactions with atomic hydrogen, this observation clearly showed that significant gas-phase chemistry was occurring. A notable feature of these results is that methane and acetylene account for the majority of the gas-phase carbon. Ethylene is present at much lower levels and ethane (C_2H_6) is not detected. The only two radical species which are detectable are atomic hydrogen and the methyl radical CH_3.

Chemical equilibrium analysis indicates that the distribution of the C_1 species is a function of only the H/H_2 ratio and the local temperature. Normally the H/H_2 ratio in a diamond CVD system is in a range of 10^{-3}-1, which leads to a result that the most abundant C_1 radicals are CH_3 and atomic carbon. Therefore, CH_3 and C are most often postulated to be important for diamond growth.

The distribution of species with the C_2 system (C_2 through C_2H_6) can not be explained by simple partial equilibriums of hydrogen shift reactions. This results from the fact that the species C_2H_2, C_2H_4, and C_2H_6 are all stable molecules, and thus reactions such as

$$C_2H_2 + H_2 \rightarrow C_2H_3 + H \qquad (8)$$

have high activation energies and are consequently very slow.

The concentrations of all C_2H_n species with $n > 2$ are generally low, since these species are thermodynamically less stable at high temperature and in the presence of atomic hydrogen than acetylene. Thus C_2H_n ($n > 2$) species are rapidly converted to acetylene. Therefore, C_2H_2 is still suggested to have a possible role in diamond growth.

3.1.3 Effect of oxygen addition

Although most diamond CVD is carried out with hydrocarbon/hydrogen gas mixtures, it is also common to add a small amount of oxygen, or an oxygen-containing compound. Several studies have reported enhanced growth rates or quality due to oxygen addition and, more importantly, the substrate temperature can be significantly lowered when oxygen is introduced into the hydrocarbon/H_2 gas mixtures [73-78].

Because of the rapid gas-phase chemistry, the equilibrium composition provides, once again, a first estimation of the effect of oxygen addition on the gas composition. Since acetylene is typically one of the most abundant hydrocarbons, let us consider the oxidation reaction

$$C_2H_2 + O_2 \leftrightarrow 2CO + H_2 \qquad (9)$$

This reaction is highly exothermic. The Gibbs free energy is highly negative, resulting in the extent of reaction near one. The reaction shifts strongly to the right, proceeding until essentially all of one reactant is depleted. Harris and Weiner [79] have reported mass spectral measurements during diamond CVD growth with various mixtures of CH_4, O_2, and H_2. In all cases, they found that adding O_2 reduced the hydrocarbon mole fractions. No O_2 was detected experimentally at the substrate, indicating that all injected O_2 was rapidly consumed. These results are also consistent with the empirical observations of Bachmann *et al.* [80]. As in the case of the acetylene/oxygen flame, for high oxygen content, solid carbon precipitation in thermodynamically not possible, because CO_2 and H_2O are more stable and the Gibbs free energy of the reaction is highly negative. At lower oxygen concentration precipitation of carbon can occur. The metastable diamond phase is detected at the borderline from no deposition to C (s) precipitation. These observations suggest that the oxygen rapidly oxidizes any available hydrocarbon. Even though the

main effect of oxygen addition is to oxidize some of the hydrocarbon to form CO and H_2, there are other effects which may be significant for the film growth. For example, it has been shown that oxygen addition can result in a slight increase in the H level and OH level [79]. Since OH can oxidize pyrolytic, non-diamond carbon, it may play a role similar to H and thus oxygen addition may aid diamond growth through creation of OH radicals.

3.2 The growth species and growth mechanisms

The question of which carbon-bearing gas-phase species is most responsible for CVD diamond growth has attracted much interest. In addition to its fundamental nature, this question is important for reactor design, since once the "growth species" is identified, a reactor could be designed to maximize the concentration of this species.

There have been many suggestions for the growth species, including small radicals (C, CH, C_2, C_2H, CH_3), ions (CH_3^+) and large hydrocarbons which have a similar structure to diamond. Some of these were suggested based on observation of characteristic emission spectra in plasma or flame environments during diamond growth. However, some species, such as C_2 and CH, may produce intense visible emission due to electron-impact excitation or chemiluminescence even at concentrations far too low to account for measured growth rates, while other abundant species (CH_3 and C_2H_2) have no prominent visible emission bands. Therefore, it is difficult to draw conclusions about the significance of a given species from its emission spectrum.

The observation that diamond may be readily grown in hot-filament reactors at rates comparable to plasma systems operating at the same pressure and flow rate indicates that species which might be found in plasma (ions, electrons, electronically-excited neutrals) but not in a "thermal" environment are probably not important for diamond CVD. For this reason, most work on determining the growth species has focused on neutral species.

It is reasonable to assume that any potential growth species must have a collision frequency with the surface at least as great as the rate at which carbon is incorporating into the film. For a typical growth

rate of 1 μm/h, this implies a growth species concentration at the surface of at least $3\times10^{10}/\sqrt{n_c}\ cm^{-3}$ (n_c is the number of carbons in the growth species) [80]. From measured concentrations of stable species, it was found that only CH_4, CH_3 and C_2H_2 are present in sufficient quantities to account for measured growth rates. When the low reactivity of methane is taken into account, only CH_3 and C_2H_2 are left as likely growth species under typical diamond CVD conditions.

Several mechanisms for diamond CVD have been proposed, including *CH_3-based mechanisms* [81,82], *Acetylene-addition mechanisms* [83], *Combined $CH_3 - C_2H_2$ mechanism* [83]. However, none of them has been generally accepted as the likely path for incorporation of gas phase carbon into a bulk diamond structure.

3.3 Diamond doping

CVD diamond p-type and n-type doping can be achieved through the addition of proper elements in the gas phase.

Boron has been widely used as a dopant for obtaining p-type diamond; boron doping can be achieved by adding substances such as diborane or trimethyl borane to the plasma. The activation energy is relatively high, 0.37 eV [84] and this corresponds to a level too deep for room temperature applications at typical doping levels. However, when the doping level reaches values higher than $10^{20}\ cm^{-3}$, the conduction mechanism changes and the activation energy approaches zero [85]. Taking advantage of this fact, high performance transistors with full activation at room temperature [86] and heavily boron-doped diamond electrodes for electrochemical applications [87] have been successfully fabricated.

Phosphorous-doped diamond yields n-type conductivity with a donor lever 0.56 eV under the conduction band [88]. Again, this level is too deep for conventional room temperature applications. The possibility of n- and p-type diamond doping opens the door for a generation of bipolar devices, such as a diamond pn junction reported by Koizumi *et al.* [89].

Other dopants have also been tried, such as sulphur and arsenic [90], however no systematic results have been obtained so far. A complex involving boron and hydrogen complex has recently been

proposed as a shallow dopant for n-type diamond [91] but the long-term stability of the complex is still not known. So far boron and phosphorous remain the most widely accepted and used diamond dopants.

As-grown CVD diamond surfaces, grown under hydrogen-rich atmospheres, also show p-type surface conductivity due to the termination of the dangling bonds with hydrogen atoms [92] and have been widely used to fabricate planar devices operating at room temperature [93].

4 CVD Diamond Characterization Techniques

Depending on the applications of the CVD diamond films, various techniques can be employed to characterize the materials microstructure and their properties, including optical, electrical, thermal and mechanical characteristics. Two most fundamental techniques, Raman spectroscopy and X-ray diffraction (XRD), are most intensively used to identify diamond films. In fact, Raman spectra could be found in almost every published paper related to CVD diamond growth. Due to their special role in characterizing diamond films, we discuss in more details about Raman and XRD in this section.

4.1 Raman spectroscopy

Raman spectroscopy is most extensively used to characterize CVD diamond because of the ability to distinguish between different forms of carbon [94-96]. In the Raman spectrometers a laser beam of certain wavelength can be focused at a spot of 1 μm. The spectrum resolution can reach 0.5 cm^{-1}. In some instruments, a confocal component is installed, which allows a depth profiling of the spectra. However, the penetrating depth of the laser into the sample depends strongly on the film quality.

It is known that atoms in a crystal vibrate at characteristic frequencies and the lattice vibrations can be visualized as quanta, called 'phonons', with energy $h\nu$, where ν is the frequency and h is Planck's constant. In Raman scattering measurement, monochromatic light with frequency ν_i interacts with phonons in the crystal having frequency ν_{phonon}. In this process a phonon can be either created or destroyed, giving rise to either the Stokes Raman line with frequency ν_i-ν_{phonon} or the anti-Stokes Raman line with frequency ν_i+ν_{phonon}. The anti-Stokes line is much weaker than the Stokes line and depends

strongly on temperature as it depends on the number of the excited vibration levels at that temperature. Therefore, at room temperature, it is the Stokes line that is normally observed for diamond. A large fraction of the incident light is Rayleigh scattered at the same frequency as the incident light. In order that this Rayleigh scattered light does not impair the Raman spectrum it is necessary to use a high-quality double monochromator, or a filter that strongly absorbs the exciting radiation but passes the Raman scattered spectrum.

In CVD films, the presence of diamond is revealed by a sharp line at 1332 cm^{-1} that is due to a vibration of the two interpenetrating cubic sub-lattices of diamond, while graphite usually gives rise to two broader peaks around 1335 cm^{-1} and 1580 cm^{-1} with similar intensity. The ratio of the intensities of the diamond peak to the graphite peak indicates how much of each phase is present, but is also dependent on the wavelength of excitation. The width of the 1332 cm^{-1} line reveals how much random stress is present, and any directional stress present may give rise to a shift or splitting of the line, as will be discussed later. The film may also contain amorphous sp^2-bonded (graphite) carbon and sp^3-bonded (diamond-like) carbon. These give rise to broad ill-defined bands with a high-frequency cut-off near 1332 cm^{-1} for the sp^3-bonded carbon, and around 1580 cm^{-1} for the sp^2-bonded carbon. Fig. 7 shows Raman spectra for two different polycrystalline CVD films deposited on copper. They were measured using a Raman spectrometer excited at 633 nm. Film (a) shows mainly the 1332 cm^{-1} diamond peak and is of better quality comparing with film (b), which exhibits broad bands, in addition to the diamond Raman peak. However, the form of the Raman spectra is greatly influenced by the wavelength of laser used for excitation. Fig. 8 shows Raman spectra taken from the same samples (a) and (b) using a Raman spectrometer excited at 514 nm. The spectra suggest that even film (b) has quite good quality. This phenomenon has been attributed to a resonance effect, in which the non-diamond forms of carbon scatter far more effectively than diamond at longer excitation wavelengths [97].

Fig. 7

Fig. 8

The message here is clear: if we are concerned with the non-diamond carbon phases or trying to produce high quality diamond, it is a much more stringent test to measure the Raman spectra with a longer wavelength laser (633 nm or longer). If we are interested in finding the diamond peak position, shorter wavelength laser may give a more accurate result.

4.2 X-ray diffraction

In addition to the Raman spectroscopy, XRD can be used to confirm that diamond synthesis has indeed been achieved. Besides identifying the presence of crystalline phases, the XRD patterns also provide information on strain, grain size, preferential orientation, etc. Fig. 11 shows XRD patterns of the two diamonds used in Fig. 7 and Fig. 8. As a reference the positions (<120 °) and relative intensities of the strongest XRD peaks for powdered diamond are given in Fig. 9 and in Table 5. It is clear that the XRD is a technique as powerful as the Raman spectroscopy since it also provides a fingerprint of the presence of diamond phase. Note that the diamond films deposited under different conditions may possess different preference growth direction. This may contribute to a variation of the relative intensity of the XRD peaks. For example, the (111) diamond peak is nearly not visible for sample (a), while its (220) peak is much more intense than in sample (b). It is worth to mention that some substrate materials, like copper, also have a cubic structure and its lattice parameter is similar to that of diamond. Since X-ray can penetrate diamond more than 100 μm, the XRD patterns usually exhibit peaks of the substrate, which are very close to those of diamond and are even stronger than diamond peaks. Special attention is needed on this. In addition, buffer layers are used in the samples to promote the adhesion of diamond to copper. The XRD is sensitive enough to reveal the structure of the buffer layers, as evidenced by those un-labelled peaks that are neither due to the diamond films nor to the copper substrates shown in Fig. 9.

Fig. 9

Table 5

5 Heteroepitaxial CVD Diamond Growth Characteristics

CVD diamond growth includes a few steps, i.e., nucleation, formation of continuous film, competition growth of crystallites. The resulting film structure, properties, and surface morphology are closely related to these three stages. In this section, we briefly discuss the effects of substrate pre-treatment on diamond nucleation, the effects of deposition conditions on CVD diamond nucleation and growth, and the growth behaviours of diamond films on various types of substrate materials.

5.1 Effect of substrate pre-treatment on diamond nucleation

The first difficulty that arises from the attempt to grow diamond on foreign substrates is that a continuous diamond film cannot be deposited unless a proper nucleation step precedes the growth. After a non-diamond substrate has been exposed to proper growth conditions without a nucleation procedure only a few isolated diamond crystallites (~10^5-10^6 cm^{-2}) will be found. The control of nucleation density and film growth is significant for different applications. For instance, a nucleation density higher than $10^8/cm^2$ is required in diamond coating on metals in order to improve adhesion and to reduce carbon diffusion into the substrate.

Different nucleation procedures have been proposed, the simplest of which is a diamond grit abrading process, where the flat substrate is pressed against a soft or hard plate that contains diamond powders from a natural or synthetic source [98]. By the end of this process, small diamond particles of sizes in the range of 2-10 nm are left on the surface and act as growth sites once the growth cycle is initiated. It is generally accepted that surface defects such as grain boundaries and dislocations are favourite sites for diamond nucleation [99]. The nucleation enhancement by scratching can be generally attributed to (a) seeding effect, (b) minimization of interfacial energy on a sharp convex surface, (c) breaking of a number of surface bonds or presence of a number of dangling bonds at sharp edges, (d) rapid carbon saturation (fast carbide formation) at sharp edges.

For many applications, this procedure is sufficiently effective. Fig. 10 shows SEM images of diamond nucleation on copper with different pre-polishing process to the substrate. The nucleation

density on copper without pre-treatment (Fig. 10a) is quite low, approximately $5x10^6/cm^2$, while diamond powder polishing leads to a significant increase in the nucleation density (Fig. 10c). However, this method has some limitations: it can be used only with flat surfaces, and if the substrate is coated with some intermediate layer (for example, by layers that are intended to prevent the film delamination) it may be damaged by the harsh abrading action.

Fig. 10

The ultrasonic treatment [100] is a gentler method, where the substrate is simply immersed in a cleaning ultrasonic bath, with the diamond powder properly dispersed in an organic solvent like methanol. This method can be used with 3D-shaped substrates and the appropriate choice of the diamond particles size and the seeding time allows a further control of the nucleation procedure. Nanodiamond particles can also be used; in this case, they can be processed to prevent agglomeration and dispersed in a colloidal solution with an appropriate solvent [101]. Nucleation densities as high as 10^{11} cm^{-2} have been obtained with this method. A modified method, known as NNP (Novel Nucleation Procedure), involves the deposition of a carbon film prior to the ultrasonic treatment by exposing the substrate to the growth conditions [102]. Besides increasing the nucleation density, this pre-deposited carbon film acts as a carbon supply and facilitates the diamond coverage of complex 3D shapes [103].

Another widely known method is the Bias Enhanced Nucleation (BEN) method [104] which employs an *in situ* surface bombardment under an applied negative bias on a conductive substrate. The applied electric field increases the ionization degree of the neutral gas molecules, the energy of the ions and the surface ion bombardment rate. Different ionic species may be involved in the bombardment, such as CH_x^+ (x = 1 to 5), C, H^+ and H_2^+ [105]. During the bombardment, the ionic species alter the surface and create surface structures that act as the seeds for the growth. The ionic species react with the substrate, resulting in the formation of a silicon carbide layer with improved adhesion when silicon is used as the substrate [106]. Nucleation densities higher than 1×10^{11} cm^{-2} have been obtained with this method [107], however, Maillard-Schaller *et al.* reported surface damage induced on a silicon substrate during the BEN

that happened in the form of holes that could be as deep as 2-3 μm and as large as 200-300 nm in diameter [108].

Once the small diamond crystallites are present on the non-diamond substrate surface by the nucleation procedure, they start growing three-dimensionally until the grains coalesce and form a continuous film; this happens during a time period known as the incubation time. The growth proceeds with competitive crystal growth between the crystals oriented along the fastest growth direction. This results in a columnar growth mode oriented parallel to the substrate, with grain sizes coarsening with the film thickness (van der Drift growth) [28].

5.2 Effect of deposition parameters on diamond nucleation and growth

The CVD process conditions have significant effects on diamond nucleation and growth. The major process parameters include input power, substrate temperature, methane concentration, gas pressure and gas flow rates. Detailed study on the effects of these deposition parameters have been systematically conducted and reported [e.g. 109,113]. The generally observed results are outlined as follows.

(1). Diamond growth rate increases with increasing microwave power, the effect of microwave power being mainly the effect of plasma density.

(2). Diamond nucleation and growth rate increase with increasing gas pressure and methane concentration. When the gas pressure reaches a certain value, e.g. 13 kPa, growth stress starts to be pronounced. The increase in the methane concentration results in monotonic increase in both growth stress and non-diamond phase.

(3). Gas flow rate has less influence on diamond nucleation and growth.

(4). The substrate temperature influences significantly the film morphology. The diamond crystals show a (111) face dominating almost in all the cases. (100) faces appear at higher substrate temperature.

Due to the importance of diamond film's morphology, we discuss it in more detail here. Most CVD diamond shows a dominant triangular (111) face. When the substrate temperature becomes

relatively high, more (100) faces appear [34,110,114]. It is known that the shape of a diamond crystal depends on the deposition conditions which may influence the relative growth rate of constituent crystallographic planes. Therefore the shapes can be used to determine the ratio of the growth rate in different directions. Fig. 11 demonstrates the variation in the crystal shape for diamond crystals supposing that the limiting faces are (100) and (111) facets but that the crystals grow at different rates $V_{<100>}$ and $V_{<111>}$ on the two types of facets. The distance from the centre of the crystal to the centre of each face is proportional to the growth rate in the direction perpendicular to that face. The longest dimension in the crystallite defines the fastest growth direction, as indicated by the arrow. It can be seen that (111) plane grows faster in a cube, while (100) plane is the fastest one in an octahedron.

Fig. 11

5.3 Substrate materials for CVD diamond films

Substrate materials used for diamond deposition may be classified into three major groups in terms of carbon-substrate interactions as listed in Table 6. According to these interactions, the materials can be classified as showing (1) little or no solubility carbon reaction, (2) strong carbon dissolving and weak carbide formation and (3) strong carbide formation. Depending on the carbon-substrate interactions, the grown diamond exhibits different interface structures and consequently different adhesion behaviours.

Table 6

In the next sections, a few examples of diamond deposition these materials are given.

5.3.1 Materials with little or no carbon solubility

The materials that have little or no C solubility or reaction include some crystals (sapphire, Ge, diamond and graphite) and a few metals such as Cu, Sn, Pb, Ag, and Au. In the case of diamond deposition on graphite substrates, the growth conditions induce the graphite etching that happens concurrently with diamond growth.

Copper can be used as an example to illustrate diamond growth on this kind of materials: as it has very low carbon affinity, the adhesion of diamond films grown on copper is expected to be very weak.

This renders copper an interesting substrate material for making free-standing diamond films. In fact, diamond film can be easily removed from the copper substrate after deposition and becomes free-standing.

Fig. 12 shows SEM images and Raman spectra of the surface and backside of the free-standing diamond film deposited on copper. It can be seen that the grain size at the film backside is much smaller than at the surface side. This is because, once the nucleation particles grow up and meet each other, they can no longer grow in the Cu surface plane but can continue the growth in a perpendicular direction. As a result of growth competition, some preferential grains become larger and larger until they reach equilibrium. The Raman spectra show a sharp peak at about 1332 cm^{-1}, indicating the existence of good diamond phase. No carbide transition layer is found, as expected. Although the diamond peaks show similar width and position, the background of the Raman spectrum of the film backside is obviously higher than that of the surface side. We suppose that this happens due to the presence of grain boundaries which are obviously in larger amount in the backside.

Fig. 12

5.3.2 Materials with strong carbon dissolving and weak carbide formation

When the materials are strong carbon dissolving, there is a considerable amount of C diffusion into the substrate during diamond growth. This class of materials includes some metals such as Pt, Pd, Rh, Fe and Ni. Under growth conditions, the substrate acts as a carbon sink and the deposited carbon dissolves into the metal surface to form a solid solution. A large amount of carbon is then transported to the bulk and this leads to a temporary decrease in the surface C concentration; this, in turn, delays the onset of nucleation.

CVD diamond coatings on steel, for instance, are attractive for mechanical applications. However, there are at least two major difficulties that hinder diamond coating on steel. First, iron is a strong carbon-dissolving element. During CVD diamond process the carbon swiftly diffuses into the steel substrate. This usually causes poor adhesion of diamond film to the steel substrate. The characteristics of the steel may also be changed due to the heavy carbon diffusion. Second, the difference in thermal expansion

coefficients between diamond and steel is very large (at room temperature, $\alpha_{diamond}$~1×10^{-6}/K, α_{steel}~16×10^{-6}/K. Both of them increase a little with temperature). This causes large residual stress in the diamond film and influences the adhesion in a negative way.

It is found that diamond film deposited directly on steel substrate can be easily removed from the steel substrate. Fig. 13 shows SEM images of the surface and backside of the diamond film grown on high speed steel MG50. The small particles in the film surface are probably some materials diffusing from the steel substrate. In the backside there is no polycrystalline structure visible. Raman spectra taken from the two sides are shown in Fig. 13. The spectrum of surface side shows a high background, which is probably due to those surface particles. The spectrum of the backside shows two broad peaks at ~1335 cm^{-1} and ~1580 cm^{-1} with similar intensity, being characteristic of graphite. The substrate surface, where the film is removed, shows a similar structure and Raman spectrum to the film backside, confirming the idea that, before the diamond starts to grow, graphite layer forms on the steel substrate. Because of this graphite layer the diamond film exhibits no adhesion. Performing a diffusion calculation, we can see that the carbon diffusion in iron is very heavy, as shown in Table 7.

Fig. 13

Table 7

A possible approach to gaining adhesion of diamond coatings on steel is the utilization of an interlayer. The feasibility of this solution has been demonstrated by Chen et al, who employed a Si interlayer and obtained adherent diamond coating on steel at relatively low deposition temperature [115]. Later Nesladek *et al.* [116,117] proposed a stress relief multilayer structure (Mo/Ag/Nb) and got good adhesion. So far, single interlayer materials that have been reported include Si, TiN, W, Mo, Ti, Cr-N etc. [118-122].

5.3.3 Materials with strong carbide formation

Materials with strong carbide formation include metals such as Ti, Nb, Ta, Cr, Mo, W and some rare earth metals. B and Si are also materials that form carbide layers, like other Si compounds such as

SiO_2, quartz and Si_3N_4. Carbide materials (for instance SiC, WC and TiC) are also particularly suitable for diamond deposition.

Silicon is widely used as a substrate for growing CVD diamond. Niobium is commonly used in boron-doped diamond-coated electrodes (with dimensions 50×100 cm^2) by the CONDIAS company for waste water treatment [123] and quartz in optical transparent electrodes [124]. The use of halogenated precursors also allowed the low-temperature deposition on low melting materials, such as glass [125].

As discussed before, titanium forms strong carbide bond as well as silicon. Therefore, diamond coating on these types of substrate materials is expected to present good adhesion. Under optimized pre-treatment and deposition conditions, adherent diamond films can be deposited on Ti substrate. Fig. 14 shows the Raman spectrum of the diamond coating. It is found that the Raman peak shifts to about 1337 cm^{-1}. It is noted that free-standing diamond films usually exhibit a Raman peak at 1332 cm^{-1} wave numbers, while the adherent films show the peak shift due to the presence of in-plane stresses caused mainly by the thermal mismatch between the substrate and the diamond film. The stress σ in the diamond film can be estimated from $\sigma = -0.567(\nu_m - \nu_0)$ (GPa) for unsplitted Raman peak at ν_m, where $\nu_0 = 1332$. Thus, the films can accommodate a compression stress of 2.835 GPa without delamination.

Fig. 14

Similarly, adherent diamond films can be deposited on Si substrate. Si has a sufficiently high melting point (1683 ^oK), it forms a localised carbide layer and it has a comparatively low thermal expansion coefficient. The stress in the film is much smaller, as evidenced by the Raman shift in Fig. 15 and Table 8. It is interesting to note that the nature of the stress changes with film growth, which implies the variation of intrinsic stress along the film depth profile. Fig. 16 shows the profile of a thick diamond film. The significant change in the size of the crystals can be clearly seen.

As diamond films with strong adhesion can be deposited on Ti and Si, these two materials are often used as interlayers for obtaining adherent diamond coatings on substrates like steel and copper.

Fig. 15

Table 8

Fig. 16

6 Nanocrystalline Diamond

In spite of the remarkable properties of diamond, the high surface roughness of CVD diamond films presents a major roadblock that prevents their widespread use in various applications [126,127], such as machining and wear, field-emission or optical applications.

In order to overcome this problem, different approaches may be followed; either a post-deposition polishing procedure or a growth cycle intended to decrease the surface roughness. Since the post-polishing is an expensive and time-consuming technique [128], a lot of effort has been devoted to decreasing the surface roughness of the CVD diamond films with a proper control of the gas chemistry and the deposition parameters. One way to obtain diamond films with considerable thicknesses (several tens of microns) and low surface roughness is to control the crystalline orientation with (100) facets that are parallel to the film plane [129]. A different and more flexible approach is the reduction of the film grain size (from micrometers to nanometers) by means of the growth chemistry and the surface temperature. These diamond films, commonly referred to as NanoCrystalline Diamond films (NCD), are grown in hydrogen-rich CVD environments and have grain sizes ranging from a few nanometers up to a hundred nanometers (increasing with the film thickness) and very low (0.1%) to high (50%) amounts of sp^2-bonded carbon, in the form of defects or grain-boundaries [130]. A second category of nanocrystalline diamond films, known as Ultra-NanoCrystalline Diamond films (UNCD), are grown in argon-rich, hydrogen-poor CVD environments, and have a typical grain size of 2-5 nm, independent of the film thickness. The nano grains are embedded in a non-diamond matrix and the films show a significant content of sp^2-bonded carbon (up to 5%) [131]. NCD and UNCD films have, in general, high Young's modulus, high hardness and a low macroscopic friction coefficient, due to their low surface roughness, and are optically transparent. The UNCD films are also electrically conductive, due to the non-diamond

matrix; both types of film can easily be doped by introducing a gas such as nitrogen or diborane into the growth chamber.

6.1 Nanocrystalline and ultrananocrystalline diamond film growth

Both NCD and UNCD are usually deposited on non-diamond substrates, such as silicon wafers. Other materials can also be used, such as SiC, SiO_2, Si_3N_4, etc. The deposition of NCD and UNCD films involves, like the CVD of the microcrystalline diamond films described above, some kind of nucleation procedure that will provide the substrate with the necessary diamond seeds for the further film growth (polishing with diamond powder, pre-coating of a carbon film, ultrasonic treatment, bias-enhanced nucleation).

6.1.1 NCD film growth

NCD films can be deposited by different methods, such as MPCVD [132-137], Electron Cyclotron Resonance [138,139], DC Glow Discharge [140,141] and HFCVD [142-146]. They are typically grown in hydrogen-rich, carbon lean environments, with surface temperatures between 250 and 1000 ºC and pressures higher than 660 Pa [130]. Some nitrogen may also be added during the growth in order to increase the electrical conductivity of the NCD and the methane-hydrogen ratio can vary between 0.1 and 4%.

NCD films deposited with a high percentage of CH_4/H_2 ratio (5–20%) usually show cauliflower- or ballas-type growth morphology [147,148] – Fig. 17a [130]; the higher amount of CH_4 in the gas phase increases the twinning and non-diamond carbon incorporation [149] (up to 50% non-sp^3 carbon), reducing the grain size. The addition of N_2 to the gas phase also reduces the NCD grain size (3–30 nm) [150,151] due to increased micro-twinning and stacking faults that result in the nanocrystalline structure [149].

They can also be deposited by bias-enhanced growth [136] under moderate (2–6%) CH_4/H_2 ratios and continuous DC bias (200–320 V) during the deposition. These films show enormous stress, ranging from 1GPa to 85GPa; apparently, the combination of surface and sub-plantation processes leads to the

formation of a mixed phase containing amorphous tetrahedral carbon and NCD, originating the high internal stress.

Deposition under extremely low (0.3%) CH_4/H_2 ratios originates the highest quality NCD films, with a low content of non-sp^3 carbon and high Young's modulus, thermal diffusivity and nucleation density [152].

Fig. 17.

6.1.2 UNCD films growth

In 1994, UNCD films were synthesized in a MPCVD system under hydrogen-poor (1%) and argon/carbon-rich conditions, using C_{60} as the carbon source [153]. Contrary to usual diamond CVD conditions, there was no excess of atomic hydrogen in the plasma, and it was proposed that the fragmentation of the C_{60} molecule due to Ar^+ collisions lead to the production of the C_2 radicals. These radicals would directly insert into the C–H bond at the diamond surface, eliminating the need for atomic hydrogen. Theoretical calculations indicated possible interaction mechanisms of C_2 on the (110) diamond surface with very low activation barriers (< 5 kcal·mol^{-1}) and the formation of a C–C bond between two adjacent absorbed C_2 being exothermic and occurring without the presence of hydrogen.

However, recent experimental measurements of the C_2 species absolute densities in $Ar/CH_4/H_2$ and $He/CH_4/H_2$ plasmas, using cavity ring down spectroscopy [154], did not detect ground-state C_2 in the $He/CH_4/H_2$ plasma; in addition, the ground-state C_2 in the $Ar/CH_4/H_2$ plasma was too low to account for the growth rate of UNCD. This suggests that, even though C_2 may play a critical role in UNCD growth, it cannot account for the bulk growth of UNCD material. More studies are needed in this topic in order to get a clear view of the UNCD growth mechanism and the role of the different chemical species.

UNCD can be typically deposited in a MPCVD system under low (1%) CH_4/Ar ratios, at a substrate temperature between 400 and 800º C – Fig. 17b [130]. Since the amount of atomic H in the plasma is very low, diamond nucleus renucleate at a very high rate, and grain coarsening does not take place, resulting in 2–5 nm diamond grains embedded in a non-sp^3 carbon matrix [155] – Fig. 17b. The

low level of atomic H also minimizes regasification of the grains, and reasonably high growth rates can be achieved with the formation of low-thickness continuous films.

6.2 Raman spectroscopy of NCD and UNCD films

Raman spectroscopy is also widely used to characterize NCD and UNCD films, however, this technique is not straightforward due to the different phases present in the films (sp^3 and sp^2 bonding). If a UV laser is used, the photon energy is shifted closer to the high gap of sp^3-bonded carbon and this problem can be somehow overcome. However, the analysis of NCD and UNCD Raman spectra becomes still more complicated since the nanocrystalline nature of the films causes the breakdown of phonon selection rules.

Fig. 18 [156] shows the UV Raman spectra of UNCD films grown under different conditions. In addition to the 1332 (sp^3-bonded carbon) and 1560 cm^{-1} (commonly assigned to the G-band, arising from the in-plane stretching modes of the sp^2-bonded carbon at the grain boundaries [157]) peaks, distinct and broad peaks can usually be seen at 1140, 1330 and 1450 cm^{-1}.

Fig. 18.

6.3 NCD and UNCD applications

The electrical and optical properties of UNCD and NCD films make them perfect candidates for various applications, such as electrochemical electrodes, cold cathode emitters, electrical insulating and dielectric passivation layers, conducting or insulating layers in MEMS and NEMS devices, support and transmission windows, etc. In addition, they possess excellent tribological properties, with hardness values close to polycrystalline films or natural diamond, improved toughness and smooth surfaces with corresponding low friction coefficients.

One of the first applications of NCD films was as support membranes for absorber patterns in X-ray photolithography and X-ray transmission windows [133,135]. More recently, they have been incorporated into silicon on insulator (SOI) wafers [157,158]. NCD-based surface acoustic wave (SAW) devices have also been fabricated, taking advantage of the improved smoothness and sound velocity of

NCD films [159]. They have also been used as an optical material to fabricate “whispering gallery” mode optical resonators [160], two dimensional photonic crystals [161,162] and UV transparent electrodes on SiC [163]. N-doped NDC films have also been used for field-emission [164] and biomedical applications [165]. Finally, different coating tools have been coated with NCD with promising results [166-168].

The tribological properties of UNCD conformal coatings were explored in different applications, such as coating seals of rotating shafts [169], monolithic AFM tips [170] and inkjets for corrosive liquids [171]. Smooth UNCD films have also been widely used as structural materials [172-178] and micromechanical switches [179,180] in MEMS and NEMS technology. Efficient field emitters [181] and field-emitting fibres [182] have also been fabricated with UNCD.

Finally, stable chemical and DNA sensing platforms have also been obtained with chemically modified NCD and UNCD diamond surfaces [183-186].

7 Summary

This paper provides a general review on the growth of CVD poly and nanocrystalline diamond, including the material properties, development history, major deposition and characterization techniques, CVD diamond nucleation and growth mechanisms, characteristics and applications.

8 Acknowledgement

The authors would like to thank Foundation for Science and Technology (Portugal), research project contract number: PTDC/EME-MFE/68042/2006 and research grant number: SFRH/BPD/24615/2005.

9 References

[1] Dolling G and Cowley R A 1966 *Proc. Phys. Soc. London* **88** 463

[2] Kulda J, Dorner B, Roessli B, Strener H, Bauer R, May T, Karch K, Pavone P and Strauch D 1996 *Solid State Commun.* **99** 799

[3] Himpsel F J, Knapp J A, VanVechten J A and Eastman D E 1979 *Phys. Review B* **20** 624

[4] Cabral Gil, Reis P, Polini R, Titus E, Ali N, Davim J P and Grácio J 2006 *Diam. Relat. Mater.* **15** 1753
Gäbler J, Schäfer L and Westermann H 2000 *Diam. Relat. Mater.* **9** 921

[5] Balmer R S, Brandon J R, Clewes S L, Dhillon H K, Dodson J M, Friel I, Inglis P N, Madgwick T D, Markham M L, Mollart T P, Perkins N, Scarsbrook G A, Twitchen D J, Whitehead A J, Wilman J J and Woolard S M 2009 *J. Phys.: Condens. Matter* **21** 364221

[6] Neto V F, Vaz R, Oliveira M S A and Grácio J 2009 *J. Mater. Proces. Technology* **209** 1085

[7] Miller A J, Reece D M, Hudson M D, Brierley C J and Savage J A 1997 *Diam. Relat. Mater.* **6** 386
Takahashi K, Illy S, Heidinger R, Kasugai A, Minami R, Sakamoto K, Thumm M and Imai T 2005 *Fusion Engin. Design* **74** 305

[8] Pace E, Pini A, Corti G, Bogani F, Vinattieri A, Pickles C S J and Sussmann R 2001 *Diam. Relat. Mater.* **10** 736

[9] Klein C A 1993 *Diam. Relat. Mater.* **2** 1024
Dore P, Nucara A, Cannavò D, De Marzi G, Calvani P, Marcelli A, Sussmann R S, Whitehead A J, Dodge C N, Krehan A J and Peters H J 1998 *Applied Optics* **37** 5731

[10] Thumm M 2001 *Diam. Relat. Mater.* **10** 1692

[11] Brandon J R, Coe S E, Sussmann R S, Sakamoto K, Spoerl R, Heidinger R and Hanks S 2001 *Fusion Eng. Des.* **53** 553

[12] Pickles C S J, Madgwick T D, Sussmann R S and Hall C E 2000 *Industrial Diamond Review*

[13] Hiscocks M P, Kaalund C J, Ladouceur F, Huntington S T, Gibson B C, Trpkovski S, Simpson D, Ampem-Lassen E, Prawer S and Butler J E 2008 *Diam. Relat. Mater.* **17** 1831

[14] Calvani P, Corsaro A, Sinisi F, Rossi M C, Conte G, Giovine E, Ciccognani W and Limiti E 2009 *Microwave Optic. Technol. Letters* **51** 2786

[15] Gurbuz Y, Kang W P, Davidson J L, Kerns Jr D V and Zhou Q 2005 *IEEE Trans Power Electron.* **20** 1

[16] Bade J P, Sahaida S R, Stoner B R, von Windheim J A, Glass J T, Miyata K, Nishimura K and Kobashi K 1993 *Diam. Relat. Mater.* **2** 816

[17] Pang L Y S, Chan S S M, Johnston C, Chalker P R and Jackman R B 1997 *Diam. Relat. Mater.* **6** 333

[18] Mildren R P, Butler J E and Rabeau J R 2008 *Opt. Express* **16** 18950

[19] Bergonzo P, Tromson D and Mer C 2006 *J. Synchrotron Radiat.* **13** 151

[20] Kang W P, Davidson J L, Wisitsora-at A, Wong Y M, Takalkar R, Holmes K and Kerns D V 2004 *Diam. Related. Mater*. **13** 1944
Ueda A, Nishibayashi Y and Imai T 2009 *Diam. Relat. Mater.* **18** 854

[21] Seelmann-Eggebert M, Meisen P, Schaudel F, Koidl P, Vescan A and Leier H 2001 *Diam. Relat. Mater.* **10** 744

[22] Rotter S Z *et al*. 2008 US Patent 7,432,132

[23] Shikata S-I 1998 *Low Pressure Synthetic Diamond Properties and Applications* ed B Dischler and C Wild (Berlin: Springer) 261

[24] Baldwin J W, Zalalutdinov M K, Feygelson T, Pate B B, Butler J E and Houston B H 2006 *Diamond Relat. Mater*. **15** 2061

[25] Fujimori N 1998 *Handbook of Industrial Diamond and Diamond Films* ed M A Prelas, G Popovici and L K Bigelow (New York:Dekker) 1129

[26] Swain G M 2004 *Thin-Film Diamond* II ed C E Nebel and J Ristein (Amsterdam: Elsevier) pp 121

[27] Yoshimura M, Honda K, Kondo T, Uchikado R, Einaga Y, Rao T N Tryk D A and Fujishima A 2002 *Diamond Relat. Mater*. **11** 67

[28] Drift AVD 1967 *Phillips Res. Rep.* **22** 267

[29] Bundy F P, Hall H T, Strong H M and Wentorf R H 1955 *Nature* **176** 51

[30] Angus J 1994 *Synthetic Diamond: Emerging CVD Science and Technology*, Ed K Spear and J Dismukes (New York: John Wiley & Sons, Inc.) pp 21-39

[31] Spitsyn B and Deryagin B 1980 *USSR patent 339.134*, author's certificate dated 10 July 1956

[32] *Handbook of Industrial Diamonds and Diamond Films* 1997, Ed M Prelas, G Popovici and L Gigelow (New York: Marcel Dekker, Inc.)

[33] Matsumoto S, Sato Y, Kamo M and Setaka N 1982 *Jpn. J. Appl. Phys.* **21** L183

[34] Matsmoto S, Sato Y, Tsutsumi M and Setaka N 1982 *J. Mater. Sci.* **17** 3106

[35] Kamo M, Sato Y, Matsumoto S and Setaka N 1983 *J. Cryst. Growth* **62** 642

[36] Matsui Y, Matsumoto S and Setaka N 1983 *J. Mater. Sci. Lett.* **2** 532

[37] Deryagin B and Fedoseev D 1976 *Sci. Am.* **233** 102

[38] Spitsyn B, Bouilov L and Deryagin B 1981 *J. Cryst. Growth* **52** 219

[39] Sawabe A and Inuzuka T 1985 *Appl. Phys. Lett.* **46** 146

[40] Sawabe A and Inuzuka T 1986 *Thin Solid Films* **137** 89

[41] Kitahama K, Hirata K, Nakamatsu H, Kawai S, Fujumori N, Imai T, Yoshino H and Doi A 1986 *Appl. Phys. Lett.* **49** 634

[42] Matsumoto S 1985 *J. Mater. Sci. Lett.* **4** 600

[43] Hirose Y, Ananuma S, Okada N and Komaki K 1989 *Diamond and Diamond-like Films Proceedings* Vol. 89-12 (*The Electrochemical Society, Pennington, NJ*), Ed J Dismukes pp 80-85

[44] Kurihara K, Dasaki K, Kawarada M and Koshino N 1988 *Appl. Phys. Lett.* **52** 437

[45] Cui J, Ma Y and Fang R 1996 *Appl. Phys. Lett.* **69** 3170

[46] Tsang R S, May P W, Cole J and Ashfold M N R 1999 *Diam. Relat. Mater*. **8** 1388

[47] Rego C A, May P W, Herderson C R, Ashfold M N R, Rosser K N and Everitt N M 1995 *Diam. Relat. Mater*. **4** 770

[48] Anthony R 1991 *Diamond and Diamond-like Films and Coatings: NATO Advanced Study Institute on Diamond and Diamond-like Films* Ed R Clausing (New York: Plenum)

[49] Stoner B R, Ma G, Wolter S D and Glass J T 1992 *Phys. Rev. B* **45** 11067

[50] Matsui Y, Yuki A, Sahara M and Hirose Y 1989 *J. Appl. Phys.* **28** 1718

[51] Marks C M, Burris H R, Grun J and Snail K A 1993 *J. Appl. Phys.* **73** 755

[52] Han Q Y, Qi T W, Lu Z P, Heberlein J and Pfender E 1991 *Proc. 2nd International Symposium on Diamond Material*s Vol. 91(8) (*The Electrochemical Society, Washington D.C.*) pp 115-122

[53] Kurihara K, Sasaki K, Kawarada M and Goto Y 1991 *Application of Diamond Films and Related Materials*, Ed Y Tzeng, M Yoshikawa, M Murakawa and A Feldman (Amsterdam: Elsevier) pp 461-466

[54] Sato Y, Kamo M and Setaka N 1987 *Proc. 8th Int. Symp. Plasma Chem.* **1** 2446

[55] Patterson D E, Chu C J, Bai B J, Xiao Z L, Komplin N J, Hauge R H and Margrave J L 1992 *Diam. Relat. Mater*. **1** 768

[56] Proffitt S, Thompson C H B, Gutierrez-Sosa A, Paris N, Singh N K, Jackman R B and Foord J S 2000 *Diam. Relat. Mater.* **9** 246

[57] Schmidt I and Benndorf C 2001 *Diam. Relat. Mater.* **10** 347

[58] Celii F G, Pehrsson P E, Wang H and Butler J E 1988 *Appl. Phys. Lett.* **52** 2043

[59] Harris S L, Weiner A and Perry T 1988 *Appl. Phys. Lett.* **53** 1605

[60] Goodwin D G and Gavillet G G 1990 *J. Appl. Phys.* **68** 6393

[61] Harris S L and Weiner A 1990 *J. Appl. Phys.* **67** 6520

[62] Chu C J, D'Evelyn M P, Hauge R H and Margrave J L 1991 *J. Appl. Phys.* **70** 1695

[63] Celii F G and Butler J E 1992 *J. Appl. Phys.* **71** 2877

[64] Corat E J and Goodwin D G 1993 *J. Appl. Phys.* **74** 2021

[65] McMaster M C, Hsu W L, Coltrin M E and Dandy D S 1994 *J. Appl. Phys.* **76** 7567

[66] Rego C A, Tsang R S, May P W, Henderson C R, Ashfold M N R and Rosser K N 1996 *J. Appl. Phys.* **79** 7264

[67] Loh K P, Foord J S and Jackman R B 1997 *Diamond Relat. Mater.* **6**, 219

[68] Ferreira N G, Corat E J, Trava-Airoldi V J and Leite N F 1998 *Diamond Relat. Mater.* **7** 272

[69] Stibbe D T and Tennyson J 1998 *New J. Phys.* **1** 2

[70] Schäfer L, Klages C P, Meier U and Kohse-Höinghaus K 1991 *Appl. Phys. Lett.* **58** 571

[71] Connel L L, Fleming J W, Chu Jr H N, Vestyck D J, Jensen E and Butler J E 1995 *J. Appl. Phys.* **78** 3622

[72] McMaster M C, Hsu W L, Coltrin M E, Dandy D S and Fox C 1995 *Diamond Relat. Mater.* **4** 1000

[73] Kawato T and Kondo K 1987 *Jpn. J. Appl. Phys.* **26** 1429

[74] Liou Y, Inspektor A, Weimer R, Knight D and Messier R 1990 *J. Mater. Res.* **5** 2305

[75] Chang C P, Flamm D L, Ibbotson D E and Mucha J A 1988 *J. Appl. Phys.* **63** 1744

[76] Mucha J A, Flamm D L and Ibbotson D E 1989 *J. Appl. Phys.* **65** 3448

[77] Kapoor S, Kelly M A, Hagstrom S B 1995 *J. Appl. Phys.* **77** 6267

[78] Dementjev A P and Petukhov M N 1997 *Diamond Relat. Mater.* **6** 486

[79] Harris S J and Weiner A M 1989 *Appl. Phys. Lett.* **55** 2179

[80] Bachmann P K, Leers D and Lydtin H 1991 *Diamond Relat. Mater.* **1** 1

[81] Tsuda M, Nakajima M and Oikawa S 1986 *J. Am. Chem. Soc.* **108** 5780

[82] Tsuda M, Nakajima M and Oikawa S 1987 *Jpn. J. Appl. Phys.* **26** L527

[83] Frenklach M and Spear K E 1988 *J. Mater. Res.* **3** 133

[84] Haenni W, Rychen P, Fryda M and Comninellis C 2004 *Thin-Film Diamond Part B, Ch. Nebel, Editor, Academic Press, Semiconductors and Semimetals series, Elsevier* 149

[85] Lagrange J-P, Deneuville A and Gheeraert E 1998 *Diamond Relat. Mater.* **7** 1390

[86] El-Hajj H, Denisenko A, Kaiser A, Balmer R S and Kohn E 2008 *Diam. Relat. Mater.* **17** 1259

[87] Kraft A 2007 *Int. J. Electrochem. Soc.* **2** 355

[88] Haenen K, Meykens K, Nesl´ adek M, Knuyt G, Stals L M, Teraji T, Koizumi S and Gheeraert E 2001 *Diamond Relat. Mater.* **10** 439

[89] Koizumi S, Watanabe K, HasegawaM and Kanda H 2001 *Science* **292** 1899

[90] Sque S J, Jones R, Goss J P and Briddon P R 2004 *Phys. Rev. Lett.* **92** 017402

[91] Chevallier J, Jomard F, Teukam Z, Koizumi S, Kanda H, Sato Y, Deneuville A and BernardM 2002 *Diamond Relat. Mater.* **11** 1566

[92] Landstrass I M and Ravi K V 1989 *Appl. Phys. Lett.* **55** 975

[93] Calvani P, Sinisi F, Rossi M C, Conte G, Giovine E, Ciccognani W and Limiti E 2009 *10th International Conference on Ultimate Integration of Silicon* 257

[94] Prawer S and Nemanich R J 2004 *Phil. Trans. R. Soc. London A* **362** 2537

[95] Ferrari A C and Robertson J 2000 *Phys. Rev. B* **61** 14095

[96] Birrell J, Gerbi J E, Auciello O, Gibson J M, Johnson J and J A Carlisle J A 2005 *Diam. Relat. Mater.* **14** 86

[97] Wagner J, Wild C and Koidl P 1991 *Appl. Phys. Lett.* **59** 779

[98] Mitsuda Y, Kojima Y, Yoshida T and Akashi K 1987 *J. Mater. Sci.* **22** 1557

[99] Liu H 1996 *Diamond Relat. Mater.* **5** 211

[100] Iijima S, Aikawa Y and Baba K 1991 *Appl. Phys. Lett.* **54** 2646

[101] Williams O A, Douhéret O, Daenen M, Haenen K, Osawa E and Takahashi M 2007 *Chem. Phys. Lett.* **44** 255

[102] Rotter S 1996 *Diam. Films Techn.* **6** 331

[103] Rotter S and Madaleno J C 2009 *J. Chem. Vapor Deposition* **15** 209

[104] Yugo S, Kanai T, Kimura T and Muto T 1991, *Appl. Phys. Lett.* **58** 1036

[105] Tsuda M, Nakajima M and Oikawa S 1986 *J. Am. Chem. Soc.* **108** 5780

[106] Stoner B R, Ma G-H M, Wolter S D and Glass J T 1992 *Phys. Rev. B* **45** 11067

[107] Arnault J-C, Saada S, Delclos S, Rocha L, Intiso L, Polini R, Hoffman A, Michaelson S and Bergonzo P 2008 *Chem. Vap. Deposition* **14** 187

[108] Maillard-Schaller E, Küttel O M, Gröning O, Agostino R G, Aebi P, Schlapbach L, Wurzinger P and Pongratz P 1997 *Phys.Rev. B* **55** 15895

[109] Muranaka Y, Yamashita H and Miyadera H 1994 *Diamond Relat. Mater.* **3** 313

[110] Lu Z P, Herberlein J and Pfender E 1992 *Plasma Chemistry and Plasma Processing* **12** 35

[111] Samlenski R, Flemig G, Brenn R, Wild C, Müller-Sebert W and Koidl P 1994 *Diam. Relat. Mater.* **3** 1091

[112] Steeds J W, Gilmore A, Bussmann K M, Butler J E and Koidl P 1999 *Diam. Relat. Mater.* **8** 996

[113] Bachmann P K, Bausen H D, Lade H, Leers D, Wiechert D U, Herres N, Kohl R and Koidl P 1994 *Diam. Relat. Mater.* **3** 1308

[114] Badzian A 1994 *Synthetic Diamond: Emerging CVD Science and Technology*, Ed K E Spear and J P Dismukes (New York: Wiley-Interscience) pp 171-184 and pp 243-299

[115] Chen H, Nielsen M L, Gold C J, Dillon R O, DiGregorio J and Furtak T 1992 *Thin Solid Films* **212** 169 (1992)

[116] Nesladek M, Spinnewyn J, Asinari C, Lebout R and Lorent R 1993 *Diamond Relat. Mater.* **3** 98

[117] Nesladek M, Asinari C, Spinnewyn J, Lebout R, Lorent R and D'Olieslaeger M 1994 *Diamond Relat. Mater.* **3** 912

[118] Weiser P S, Prawer S, Hoffman A, Manory R R, Paterson P J K and Stuart S-A 1992 *J. Appl. Phys.* **72** 4643

[119] Spinnewyn J, Nesladek M and Asinari C 1993 *Diamond Relat. Mater.* **2** 361

[120] Kawarada M, Kurihara K and Sasaki K 1993 *Diamond Relat. Mater.* **2** 1083

[121] Fan Q H, Grácio J and Pereira E 1998 *Diamond Relat. Mater.* **7** 603

[122] Glozman O and Hoffman A 1998 *Diam. Relat. Mater.* **6** 796

[123] Fryda M, Matthée Th, Mulcahy S, Hampel A, Schäfer L and Tröster I 2003 *Diam. Relat. Mater.* **12** 1950

[124] Martin H B and Morrison P W 2001 *Electrochem. Solid-State Lett.* **4** E17

[125] Schmidt I and Benndorf C 2001 *Diam. Relat. Mater.* **10** 347

[126] Kamo M, Sato Y, Matsumoto S and Setaka N 1983 *J. Cryst. Growth* **62** 642

[127] Gangopadhyay A K and Tamor M A 1993 *Wear* **169** 221

[128] Choi S K, Jung D Y, Kweon S Y and Jung S K 1996 *Thin Solid Films* **279** 110

[129] Wild C, Koidl P, Muller-Sebert W, Walcher H, Kohl R, Herres N, Locher R, Samlemski R and Brenn R 1993 *Diamond Relat. Mater.* **2** 158

[130] Butler J E and Sumant A V 2008 *J. Chem. Vapor Deposition* **14** 145

[131] Gruen D M 1999 *Annu. Rev. Mater. Sci.* **29** 211

[132] Ong T P and Chang R P H 1989 *App. Phys. Lett.* **55** 2063

[133] Windischmann H 1990 *SPIE* **1263** 241

[134] Brooks C J, Powers L A, Acosta R E, Moily D, Faili F and Herb J A 1999 *J. Vac. Sci. Technol. B* **17** 3144

[135] Schafer L, Bluhm A, Klages C P, Lochel B, Buchmann L M and Huber H L 1993 *Diamond Relat. Mater.* **2** 1191

[136] Sharda T, Umeno M, Soga T and Jimbo T 2000 *Appl. Phys. Lett.* **77** 4304

[137] Celii F G, White D and Purdes A J 1992 *Thin Solid Films* **212** 140

[138] Eddy C R, Sartwell B D and Youchison D L 1991 *Surf. Coat. Technol.* **48** 69

[139] Youchison D L, Eddy C R and Sartwell B D 1993 *J. Vac. Sci. Technol. A* **11** 1875

[140] Heiman A, Gouzman I, Christiansen S H, Strunk H P and Hoffman A 2000 *Diamond Relat. Mater.* **9** 866

[141] Gouzman I, Fuchs O, Lifshitz Y, Michaelson S and Hoffman A 2007 *Diamond Relat. Mater.* **16** 762

[142] Hao T L, Zhang H, Shi C R, Han G R 2006 *Surf. Coat. Technol.* **201** 801

[143] Aikawa Y and Baba K 1993 *Jpn. J. Appl. Phys.* **32** 4680

[144] Chakk Y, Brener R and Hoffman A 1995 *Appl. Phys. Lett.* **66** 2819

[145] Kulisch W, Malave A, Lippold G, Scholz W, Mihalcea C and Oesterschulze E 1997 *Diamond Relat. Mater.* **6** 906

[146] Guillen F J H, Janischowsky K, Ebert W and Kohn E 2004 *Phys. Status Solidi A* **201** 2553

[147] Lifshitz Y, Lee C H, Wu Y, Zhang W J, Bello I and Lee S T 2006 *Appl. Phys. Lett.* **88** 243114

[148] Soga T, Sharda T and Jimbo T 2004 *Physics of the Solid State* **46** 720

[149] Butler J E and Oleynik I 2008 *Philos. Trans. R. Soc. London A - Math. Phys. Eng. Sci.* **366** 295

[150] Trolio L M, Owens M S, Butler J E, Shirey L and Wells G M 1995 *Third Int. Conf. Appl. Diamond Films Relat. Mater.* (*Gaithersburg MD*) 133

[151] Corvin R B, Harrison J G, Catledge S A and Vohra Y K 2002 *Appl. Phys. Lett.* **80** 2550

[152] Philip J, Hess P, Feygelson T, Butler J E, Chattopadhyay S, Chen K H and Chen L C 2003 *J. Appl. Phys.* **93** 2164

[153] Butler J E and Woodin R L 1993 *Phil. Trans. Roy. Soc. London A - Math. Phys. Eng. Sci.* **342** 209

[154] John P, Rabeau J R and Wilson J I B 2002 *Diamond Relat. Mater.* **11** 608

[155] Qin L C, Zhou D, Krauss A R and Gruen D M 1998 *Nanostruct. Mater.* **10** 649

[156] Birrell J, Gerbi J E, Auciello O, Gibson J M, Johnson J and Carlisle J A 2005 *Diamond Relat. Mater.* **14** 86

[157] Aleksov A, Gobien J M, Li X, Prater J T and Sitar Z 2006 *Diamond Relat. Mater.* **15** 248

[158] Feygelson T, Hobart K, Ancona M, Kub F J and Butler J E 2005 *Semicond.Wafer BondingVIII: Sci. Technol. Appl.* (*Quebec Canada*) p. 439

[159] Lee Y C, Lin S J, Buck V, Kunze R, Schmidt H, Lin C Y, Fang W Land Lin I N 2008 *Diamond and Rel. Mater.* **17** 446

[160] Wang C F, Choi Y S, Lee J C, Hu E L, Yang J and Butler J E 2007 *Appl. Phys. Lett.* **90** 081110

[161] Baldwin J W, Zalalutdinov M, Feygelson T, Butler J E and Houston B H 2006 *J. Vac. Sci. Technol. B* **24** 50

[162] Wang C F, Hanson R, Awschalom D D, Hu E L, Feygelson T, Yang J and Butler J E 2007 *Appl. Phys. Lett.* **91** 201112

[163] Tadjer M J *et al* 2007 *Appl. Phys. Lett.* **91** 163508

[164] Corvin R B, Harrison J G, Catledge S A and Vohra Y K 2002 *Appl. Phys. Lett.* **80** 2550

[165] Subramanian K, Kang W P, Davidson J L, Wong Y M and Choi B K 2007 *Diamond Relat. Mater.* **16** 1408

[166] Hu J, Chou Y K and Thompson R G 2008 *Int. J. Refract. Metals Hard Mater.* **26** 135

[167] Salgueiredo E, Almeida F A, Amaral M, Fernandes A J S, Costa F M, Silva R F and Oliveira F J 2009 *Diamond Relat. Mater.* **18** 264

[168] Ma Y P, Sun F H, Xue H G, Zhang Z M and Chen M 2007 *Diamond Relat. Mater.* **16** 481

[169] Sumant A V, Krauss A R, Gruen D M, Auciello O, Erdemir A, Williams M, Artiles A F and Adams W 2005 *Tribol. Trans.* **48** 24

[170] Pacheco S, Zurcher P, Young S R, Weston D, Dauksher W J, Auciello O, Carlisle J, Kane N and Birrell J 2005 *13th GAAS Symposium* (*Paris*) p. 2005

[171] Muller R, Gronmaier R, Janischowsky K, Kusterer J and Kohn E 2005 *Diamond Relat. Mater.* **14** 504

[172] Kohn E, Adamschik M, Schmid P, Ertl S and Floter A 2001 *Diamond Relat. Mater.* **10** 1684

[173] Kusterer J, Schmid P and Kohn E 2006 *New Diamond Frontier Carbon Technol.* **16** 295

[174] Muller R, Gronmaier R, Janischowsky K, Kusterer J and Kohn E 2005 *Diamond Relat. Mater.* **14** 504

[175] Jing W, Butler J E, Feygelson T and Nguyen C T C 2004 *17th IEEE Int. Conf. Micro Electro Mechanical Systems* p. 641

[176] Sekaric L, Parpia J M, Craighead H G, Feygelson T, Houston B H and Butler J E 2002 *Appl. Phys. Lett.* **81** 4455

[177] Hutchinson A B, Truitt P A, Schwab K C, Sekaric L, Parpia J M, Craighead H G and Butler J E 2004 *Appl. Phys. Lett.* **84** 972

[178] Baldwin J W, Zalalutdinov M K, Feygelson T, Pate B B, Butler J E and Houston B H 2006 *Diamond Relat. Mater.* **15** 2061

[179] Kusterer J, Alekov A, Pasquarelli A, Muller R, Ebert W, Lehmann-Horn F and Kohn E 2005 *Diamond Relat. Mater.* **14** 2139

[180] Schmid P, Adamschik M and Kohn E 2003 *Semicond. Sci. Technol.* **18** S72

[181] Hajra M, Hunt C E, Ding M, Auciello O, Carlisle J and Gruen D M 2003 *J. Appl. Phys.* **94** 4079

[182] Madaleno J C, Singh M K, Titus E, Cabral G and Grácio J 2008 *Appl. Phys. Lett.* 92 023113

[183] Yang W S *et al* 2002 *Nature Mater.* **1** 253

[184] Yang W S, Butler J E, Russell J N and Hamers R J 2004 *Langmuir* **20** 6778

[185] Yang W S, Baker S E, Butler J E, Lee C S, Russell J N, Shang L, Sun B and Hamers R J 2005 *Chem. Mater.* **17** 938

[186] Yang W S, Butler J E, Russell J N and Hamers R J 2007 *Analyst* **132** 296

10 Figure Captions

Fig. 1. Structure of diamond.

Fig. 2. A schematic diagram of filament-assisted CVD apparatus [30].

Fig. 3. A schematic diagram of microwave-plasma CVD apparatus [30].

Fig. 4. A schematic diagram of combustion-flame-assisted CVD set-up [30].

Fig. 5. A schematic diagram of a dc plasma jet CVD apparatus [30].

Fig. 6. Schematic of processes occurring during diamond CVD.

Fig. 7. Raman spectra of two different diamond films deposited on copper. Excitation laser wavelength is 633 nm.

Fig. 8. Raman spectra taken from the samples used in Fig. 7. Excitation laser wavelength is 514 nm.

Fig. 9. XRD patterns of two different diamond coatings on copper.

Fig. 10. SEM images of diamond nucleation on copper substrate with different polishing treatments. (a) No pretreatment. (b) Polished with Al_2O_3 powder. (c) Polished with diamond powder.

Fig. 11. Variation in the crystal shape by the growth ratio of (100) face to (111) face.

Fig. 12. SEM images and Raman spectra of the free-standing diamond film prepared by the two-step growth method. (a) film surface side, (b) film back side, (c) Raman spectra taken from the two sides under identical conditions. Wavelength of the laser source: 633 nm.

Fig. 13. Diamond film grown directly on steel at a microwave power of 2500 W for 5 hrs. SEM images show the film surface side (a) and backside (b). Raman spectra taken from the two sides are shown in (c).

Fig. 14. Raman spectrum of the diamond film grown on Ti at 2100 W for 3 hrs.

Fig. 15. Raman spectra taken from diamond films grown on 0.3 mm-thick Si substrates. The film thickness is (a) 1.7 μm, (b) 4.0 μm, (c) 11 μm, (d) 23 μm, and (e) 48 μm.

Fig. 16. SEM image of the profile of a thick diamond film.

Fig. 17. SEM image of (a) NCD and (b) UNCD. *J.E. Butler and A.V. Sumant, The CVD of Diamond Materials, Journal of Chemical. Vapor Deposition 2008, 14, pp. 152. Copyright Wiley-VCH Verlag GmbH & Co. KGaA. Reproduced with permission.*

Fig.18. UV Raman spectra of UNCD thin films grown with successive amounts of hydrogen added to the plasma. *Reproduced with permission from [156], Elsevier*.

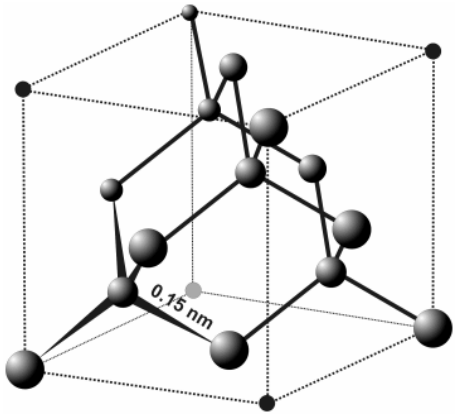

Fig. 1. Structure of diamond.

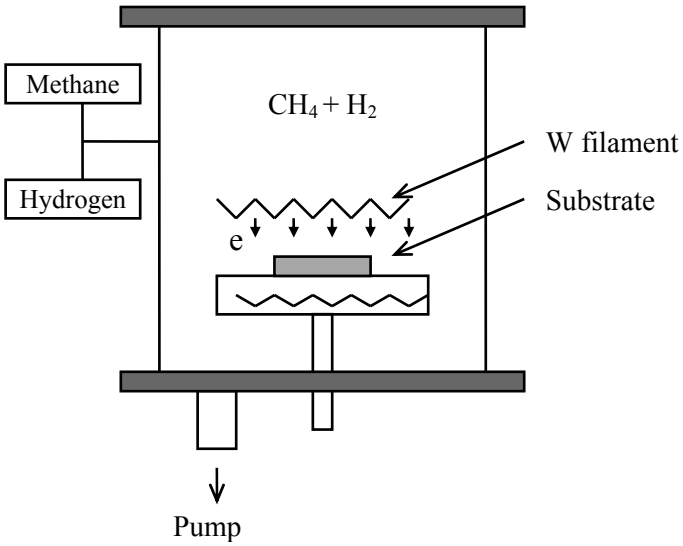

Fig. 2. A schematic diagram of filament-assisted CVD apparatus [30].

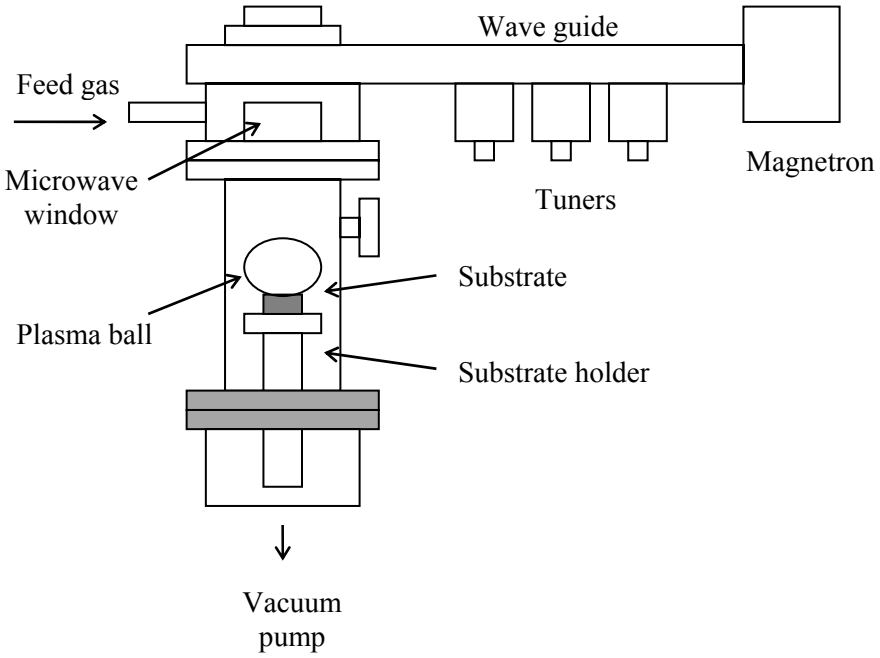

Fig. 3. A schematic diagram of microwave-plasma CVD apparatus [30].

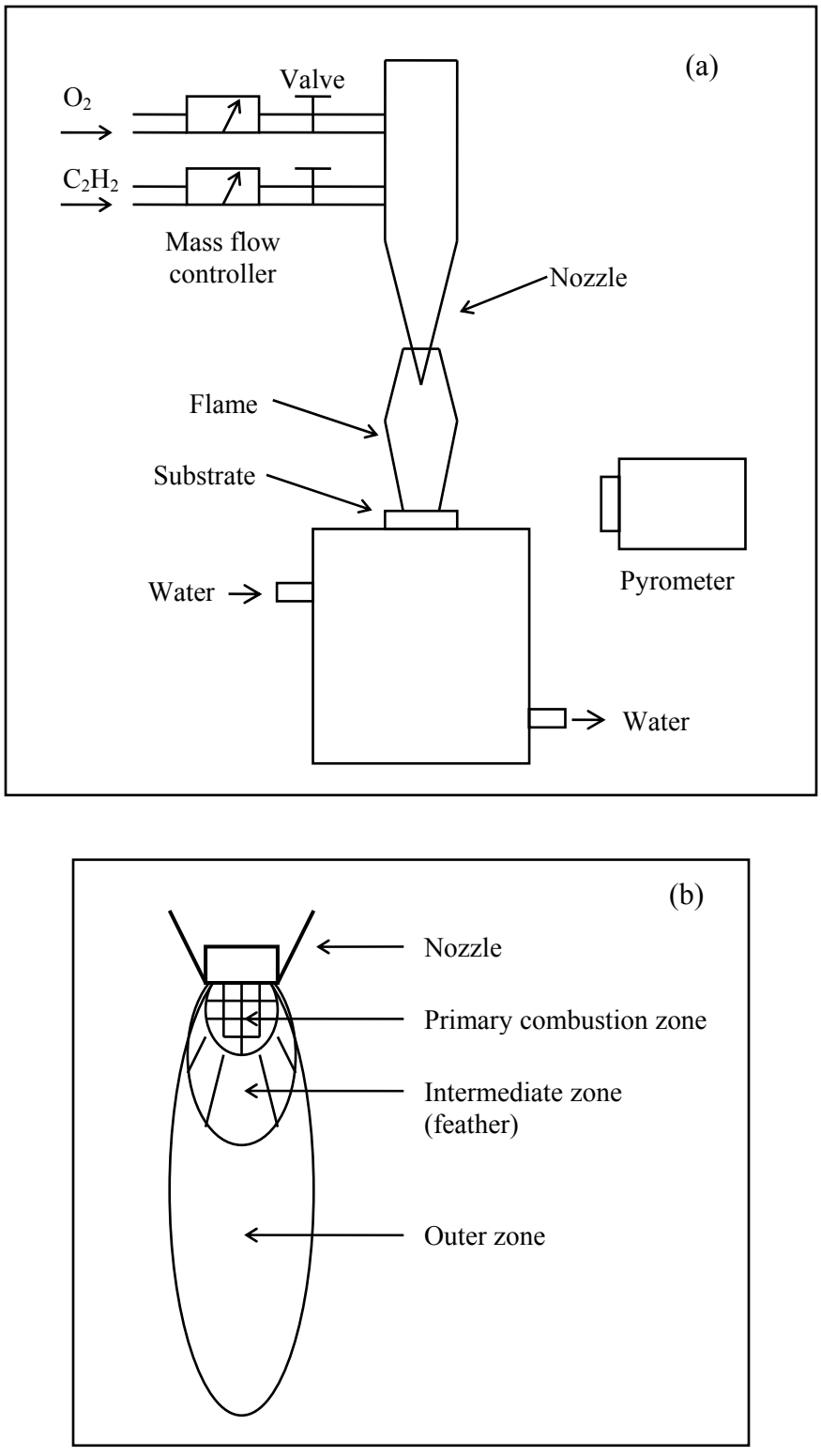

Fig. 4. (a) A schematic diagram of the combustion-flame-assisted CVD set-up [30]. (b) The combustion regions in an oxygen-acetylene flame.

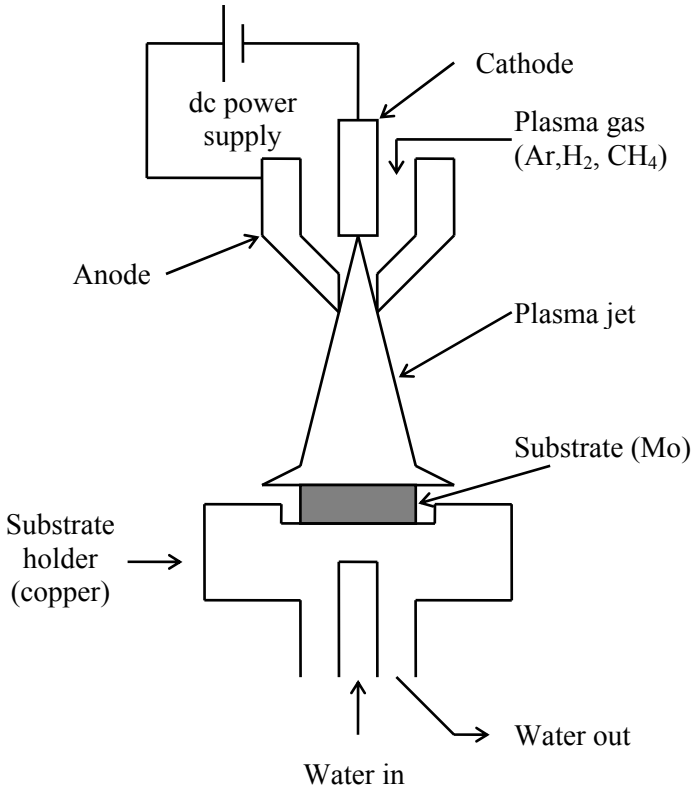

Fig. 5. A schematic diagram of a dc plasma jet CVD apparatus [30].

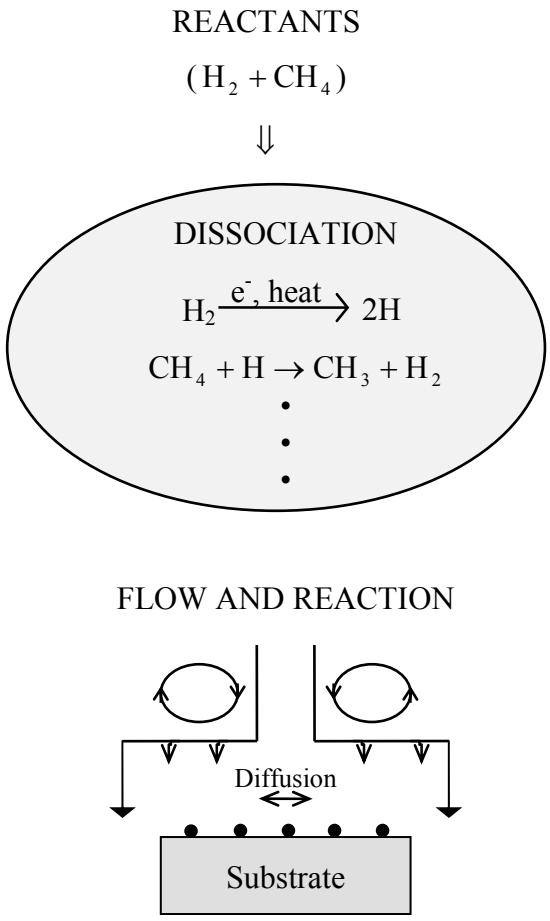

Fig. 6. Schematic of processes occurring during diamond CVD.

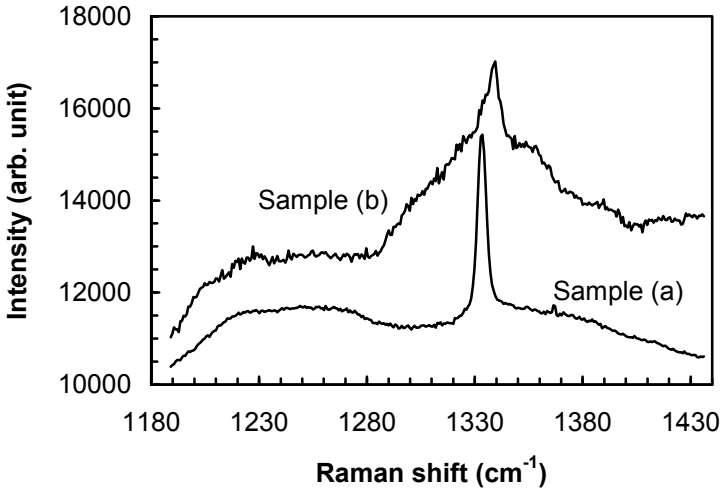

Fig. 7. Raman spectra of two different diamond films deposited on copper. Excitation laser wavelength 633 nm.

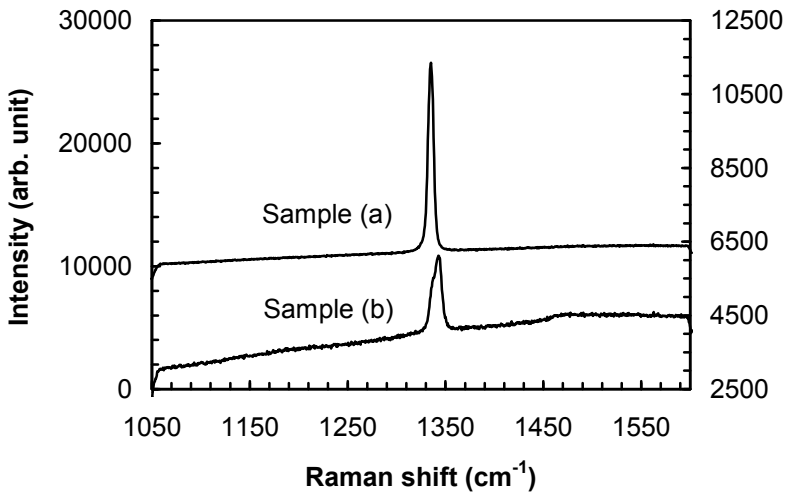

Fig. 8. Raman spectra taken from the samples used in Fig. 7. Excitation laser wavelength 514 nm.

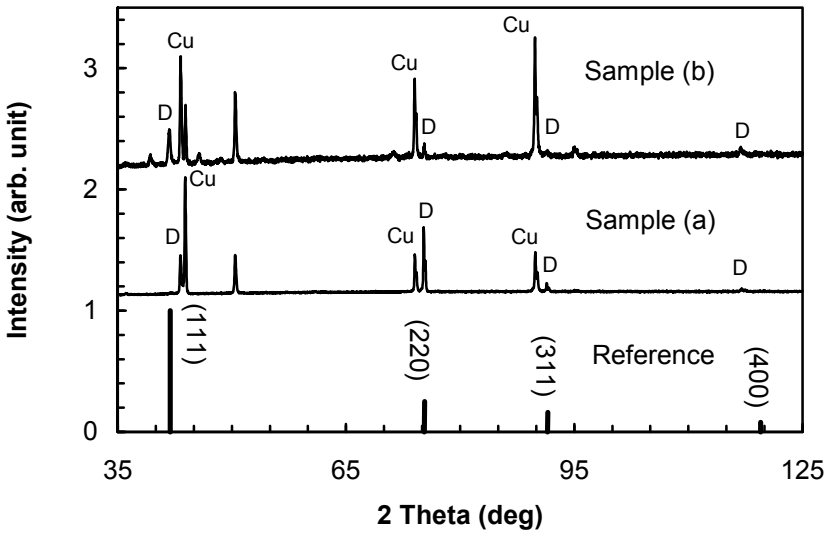

Fig. 9. XRD patterns of two different diamond coatings on copper.

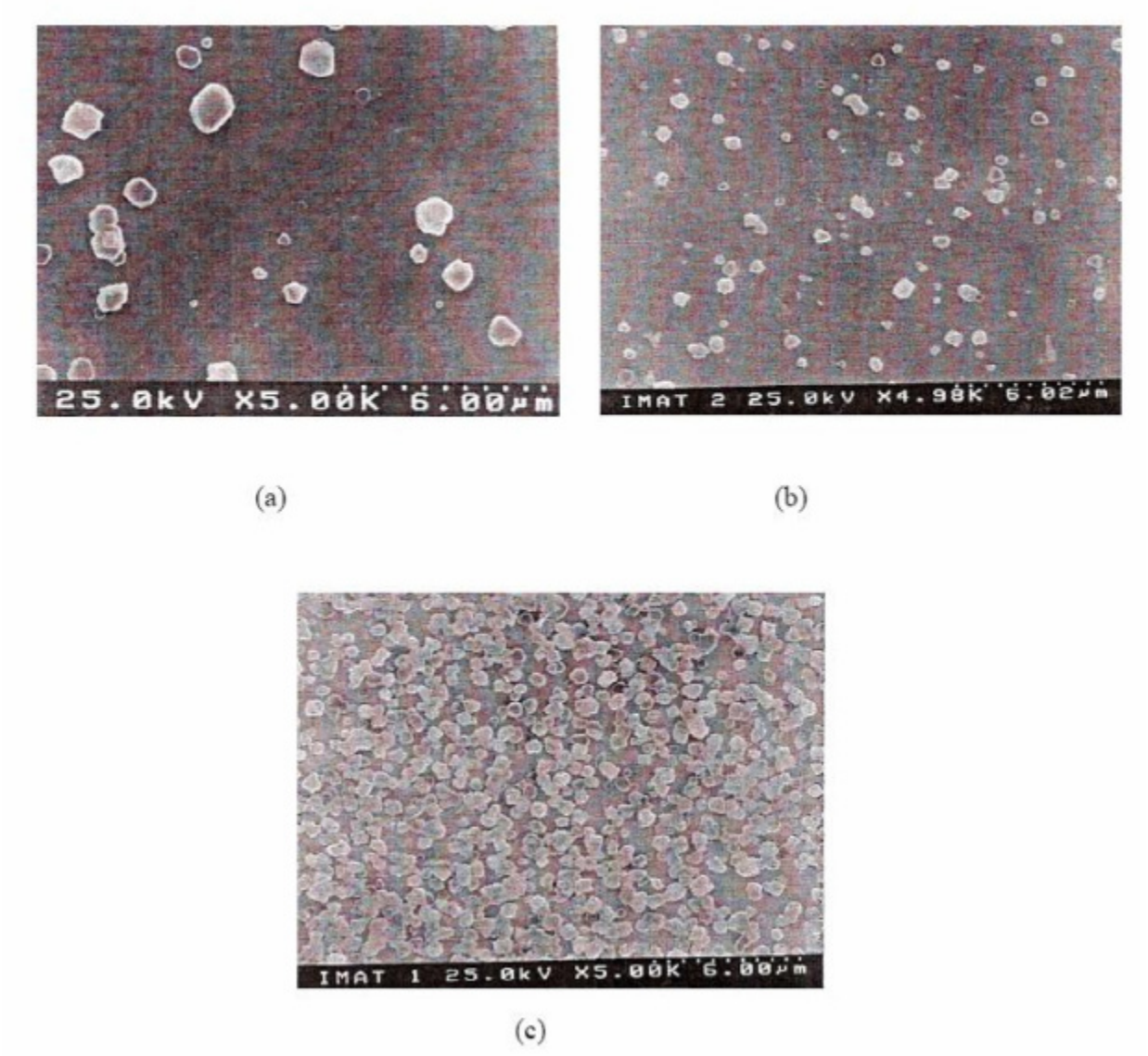

Fig. 10. SEM images of diamond nucleation on copper substrate with different polishing treatments. (a) No pretreatment. (b) Polished with Al_2O_3 powder. (c) Polished with diamond powder.

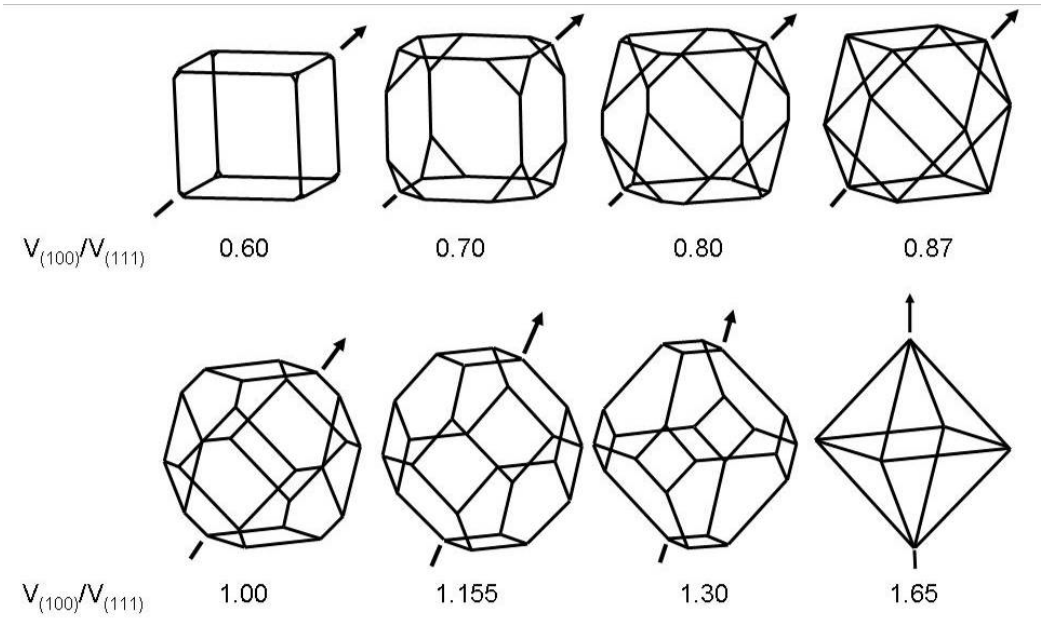

Fig.11. Variation in the crystal shape by the growth ratio of (100) face to (111) face.

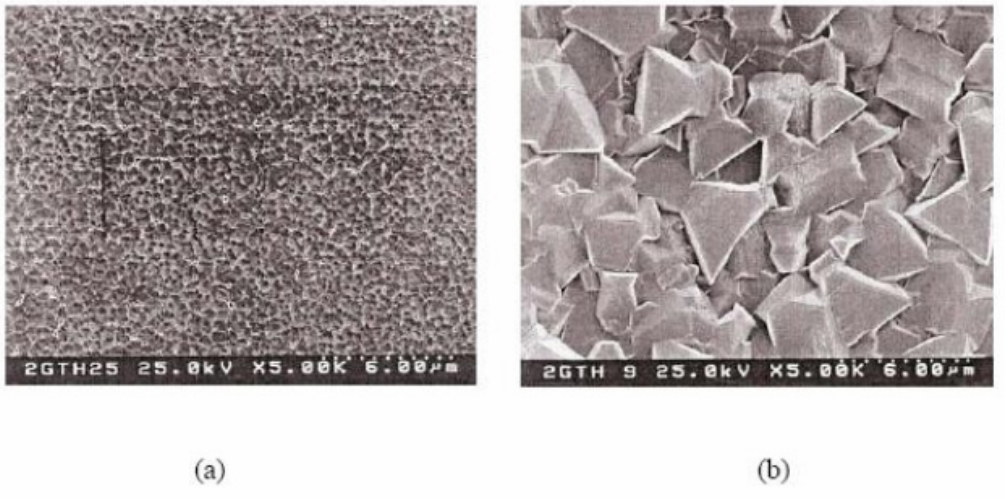

Fig. 12. SEM images and Raman spectra of the free-standing diamond film prepared by the two-step growth method. (a) film surface side, (b) film back side, (c) Raman spectra taken from the two sides under identical conditions. Wavelength of the laser source: 633 nm.

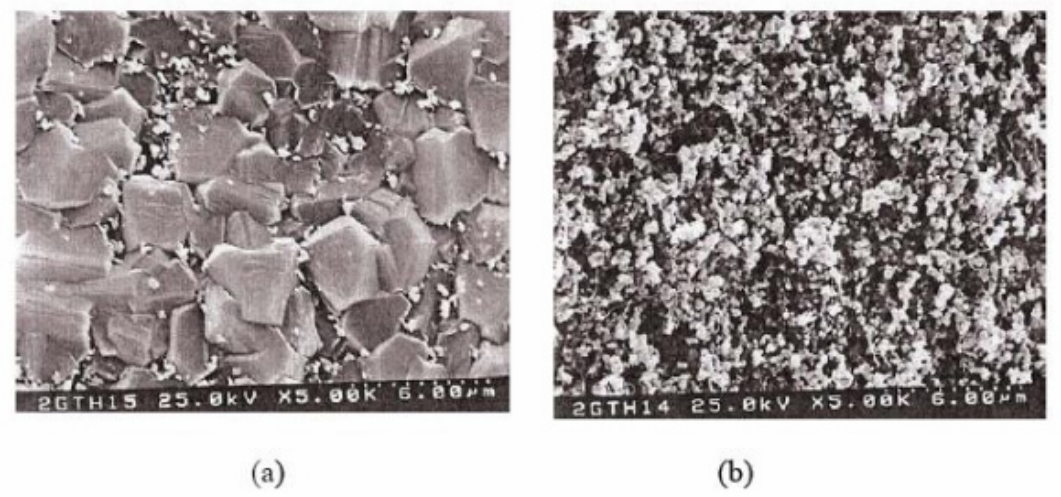

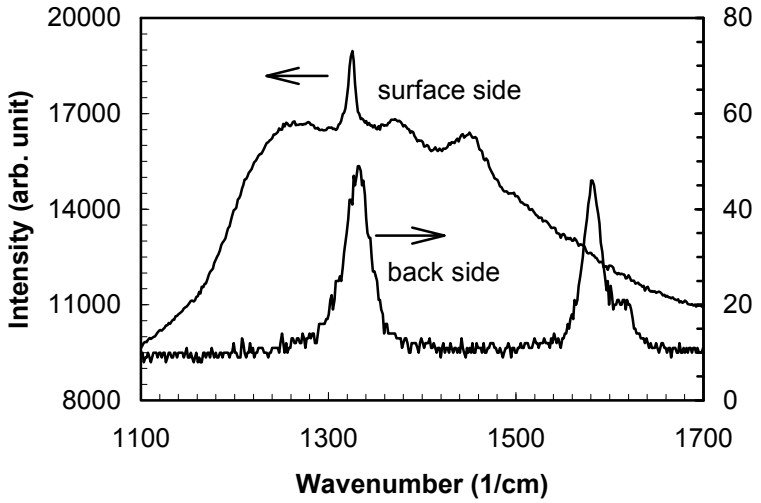

(c)

Fig. 13. Diamond film grown directly on steel at a microwave power of 2500 W for 5 hrs. SEM images show the film surface side (a) and backside (b). Raman spectra taken from the two sides are shown in (c).

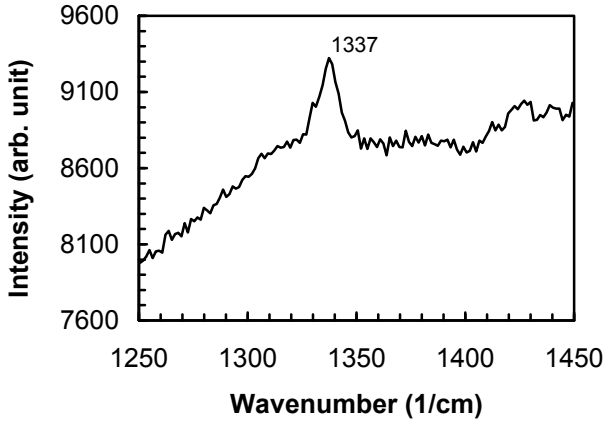

Fig. 14. Raman spectrum of the diamond film grown on Ti at 2100 W for 3 hrs.

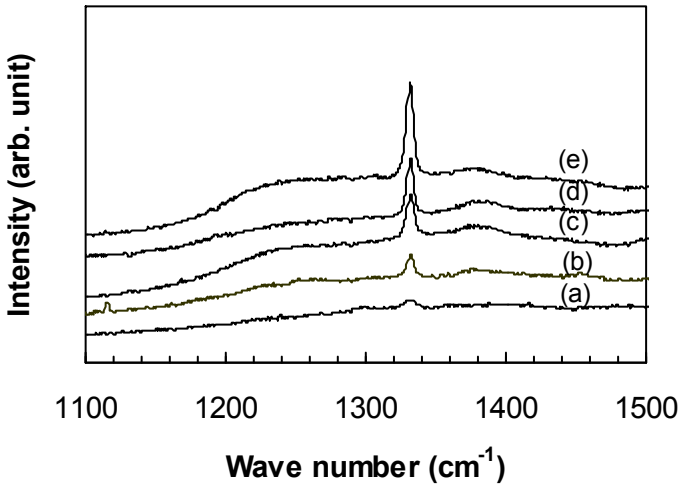

Fig. 15. Raman spectra taken from diamond films grown on 0.3 mm-thick Si substrates. The film thickness is (a) 1.7 μm, (b) 4.0 μm, (c) 11 μm, (d) 23 μm, and (e) 48 μm.

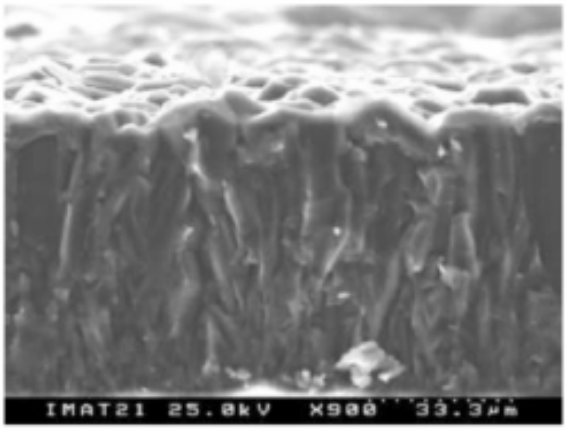

Fig. 16. SEM image of the profile of a thick diamond film.

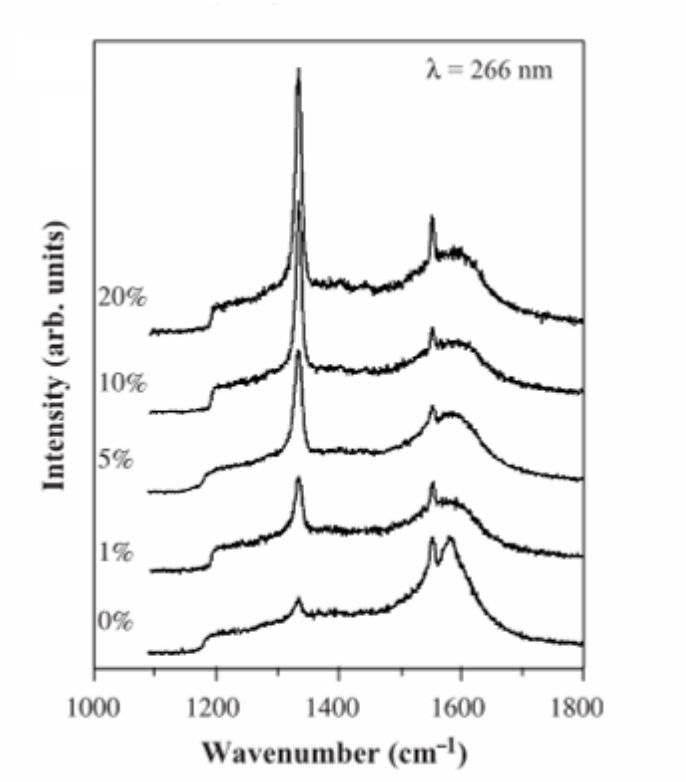

Fig. 18. UV Raman spectra of UNCD thin films grown with successive amounts of hydrogen added to the plasma. *Reproduced with permission from [156], Elsevier.*

11 Table Captions

Table 1. Outstanding properties of diamond.

Table 2. Properties and application areas of CVD diamond.

Table 3. Parameter range for diamond synthesis by filament-assisted thermal CVD method [30].

Table 4. Present status of low pressure diamond CVD methods.

Table 5. XRD patterns for powdered diamond (Cu Kα radiation, λ=1.5405 Å).

Table 6. Classification of metal substrates for CVD diamond.

Table 7. Diffusion depth *p* of carbon in iron, where the concentration C(p,T) of carbon is one thousandth of its value C(0,T). Diffusion temperature is 1100 K.

Table 8. Raman shift and corresponding residual stress in diamond films of different thickness deposited on Si substrates. The Raman shift is an average value of five different points in each sample.

Table 1. Outstanding properties of diamond.

1. Extreme mechanical hardness (~100 GPa).
2. Strongest known material, highest bulk modulus (1.2×10^{12} N/m^2).
3. Highest known value of thermal conductivity at room temperature (2×10^3 W/m·K).
4. Thermal expansion coefficient at room temperature (0.8×10^{-6} /K) comparable with that of invar.
5. Broad optical transparency from the deep UV to the far IR region of the electro-magnetic spectrum.
6. Good electrical insulator (room temperature resistivity ~10^{16} Ω·cm).
7. Very resistant to chemical corrosion.
8. High radiation hardness.
9. High bandgap (5.47 eV).
10. High breakdown field (~2×10^7 V/cm).
11. High carrier mobility (2400 cm^2/(V·s) for electrons, 2100 cm^2/(V·s) for holes.

Table 2. Properties and application areas of CVD diamond.

Property		Comments and competing materials	Possible applications
Vicker's hardness (kg/mm^2)	12000-15000	As hard as bulk diamond	Drill bits, polishing materials, cutting tools, sintered or brazed diamond compacts, wear resistant coatings on windows and moulds and bearing under vacuum
Friction coefficient	~0.1 (in air)	Depends on the grain size	
Young's modulus (N/m^2)	1.2×10^{12}	Twice the value of alumina, high mechanical strength	Stiff membrane for lithography masks, tweeter components, micromechanical oscillators
Sound propagation velocity (km/s)	18.2	1.6x the value of alumina	SAW filters
Chemical inertness	Inert	At room temp. resistant to all acids bases and solvents	Coating for reactor vessels, diamond containers, diamond electrodes
Range of high transmittance (μm)	0.22-0.25 and >6	In the IR orders of magnitude lower than other materials;	UV-VIS-IR windows and coatings, microwave windows, optical filters, optical wave guides
Refractive index	2.41	1.6x the value of silica	
Band gap (eV)	5.47	1.1 for Si; 1.43 for GaAs; 3 for B-SiC	High power electronics, high frequency devices, high temperature devices, solid-state detectors
Electron/hole mobility ($cm^2/V\cdot s$)	2400/2100	1500/600 for Si 8500/400 for GaAs	
Dielectric constant	5.5	11 for Si 12.5 for GaAs	
Thermal conductivity ($W/cm\cdot K$)	20	~4x the value of Cu or Ag	Heat sinks for electronic devices, heat spreading films on RF devices, laser packages
Thermal expansion coef. (1/K)	0.8×10^{-6}	At room temp. close to silica value of 0.57×10^{-6}	Thermal stable substrates, e.g. for x-ray lithography masks
Work function	Negative	The vacuum level lies below the conduction band	Light emitters, displays

Table 3. Parameter range for diamond synthesis by filament-assisted thermal CVD method [30].

Gas mixture	Total pressure (Torr)	Temperature (°C)	
		Substrate	Filament
H_2 + CH_4 (0.5-2%)	10-100	700-1000	2000-2300

Table 4. Present status of low pressure diamond CVD methods.

Method	Results					
	Rate (μm/h)	Area (cm^2)	Quality (Raman)	Substrates	Advantages	Drawbacks
Combustion flame	30-100	<2	+ +	Si, Mo, TiN	Simple	Area, stability
Hot filament	0.5-8	>250	+ + +	Si, Mo, silica etc.	Simple, large area	Contaminations, stability
DC plasma jet	930	<2	+ + +	MO, Si	Rate, quality	Contamination, homogeneity, stability
Microwave plasma	3 (low *P*) 30 (high *P*)	100	+ + +	Si, Mo, silica, WC, Cu etc.	Quality, stability	Rate, area
DC discharge (low *P*)	<0.1	70	+	Si, Mo, silica etc.	Simple, large area	Quality, rate
DC discharge (medium pressure)	20-250	<2	+ + +	Si. MO, alumina	Rate, quality	Area
RF plasma (thermal, 1 atm)	180	3	+ + +	Mo	Rate, quality	Area, stability, homogeneity
Microwave plasma (ECR 2.45GHz)	0.1	100	- / +	Si	Area, low *P*, low *T*	Quality, rate, contaminations

Table 5. XRD patterns for powdered diamond (Cu Kα radiation, λ=1.5405 Å).

hkl	2θ	relative intensity
111	43.9	100
220	75.3	25
311	91.5	16
400	119.5	8

Table 6. Classification of metal substrates for CVD diamond.

1. Little or no solubility or reaction	Cu, Sn, Pb, Ag, Au, etc
2. Strong carbon dissolving and weak carbide formation	Pt, Pd, Rh, Fe, Ni
3. Strong carbide formation	Si, Nb, Ta, Cr, Mo, W, etc.

Table 7. Diffusion depth p of carbon in iron, where the concentration C(p,T) of carbon is one thousandth of its value C(0,T). Diffusion temperature is 1100ºK.

Diffusion time (min)	5	10	30
Diffusion depth (μm)	804	1138	1971

Table 8. Raman shift and corresponding residual stress in diamond films of different thickness deposited on Si substrates. The Raman shift is an average value of five different points in each sample.

Film thickness (μm)	Raman shift (cm^{-1})	Stress evaluated from Raman shift (GPa)
1.7	1332.43	-0.244
4	1332.33	-0.189
11	1331.93	0.038
23	1331.73	0.151
48	1331.60	0.227